UNIVERSIDADE DA CORUÑA

Facultade de Ciencias

Grao en Química

Memoria do Traballo de Fin de Grao

Study of composites using mussel's shells in concretes for 3D-printing

Estudio de materiales compuestos usando cáscaras de mejillón para la impresión 3D

Estudio de materiais compostos usando cáscara de mexillón para a impresión 3D

Iria Rouco Olalla

Curso: 2020 - 2021.

Convocatoria: 2º/09

Directores: Socorro Castro García

Belén González Fonteboa

Agradecimientos.

Agradecer a mi tutora Suqui, por enseñarme lo que sé de ciencia de materiales y ayudarme en todo el proceso de este TFG. También a mi otra tutora Belén, que me adentró en el mundo de la construcción y me ha aportado muchos nuevos conocimientos.

A todo el grupo de investigación “gCONS” de la Escuela Técnica Superior de Ingeniería de Caminos, Canales y Puertos de la UDC que me ayudó desinteresadamente cuando lo necesitaba en el laboratorio. Cabe mencionar a María que, sin ella, habría sido impensable llevar a cabo toda la parte experimental de este TFG.

Por último, dar las gracias a mi familia y amigos que me apoyaron y no dejaron que me desanimara en ningún momento.

Index

1. Abstract/Resumen/Resumo.

1.1 Abstract.

This work focuses on the study of a type of composite material, formed by a mortar and mussel shell sand (as aggregate) in its composition, in order to investigate if it accomplishes the requirements to be 3D printable by extrusion for use in the field of construction. The mussel shell was chosen due to the large amount of this type of waste generated in Galicia, which cannot be easily used for other applications.

The present work contains a bibliographic revision of each of the components of the mortar, the reactions that take place in the formation of the mortar and the characteristics necessary to have a 3D printable mortar. Besides, a revision about the composition, morphology and microstructure of mussel shell, as well as previous experiments related to the introduction of mussel shells into building materials, was realized.

The design and preparation of a series of mixes of i) conventional mortar and ii) mortar incorporating mussel shell as aggregate, were part of the experimental work. The characterization of the mussel shell used in these mixtures was carried out and, finally, different mechanical tests were carried out comparing both types of mortars.

Comparing the prepared conventional and mussel shell mortars, it is concluded that both present a similar behavior for 3D printing. Therefore, mussel shell can be used in future mortar 3D printing experiments, although the presence of organic matter and the shape of the mussel shell particles cause the mortar to have slightly lower flowability and green strength.

1.2 Resumen.

Este trabajo se centra en el estudio de un tipo de material compuesto (composite), formado por un mortero y arena de concha de mejillón (como árido) en su composición, con el fin de investigar si cumple los requisitos para ser imprimible en 3D por extrusión para su uso en el campo de la construcción. La elección de la concha de mejillón se debe a la gran cantidad de este tipo de residuos que se generan en Galicia y que no pueden ser fácilmente aprovechados para otras aplicaciones.

El presente trabajo contiene una revisión bibliográfica de cada uno de los componentes del mortero, las reacciones que tienen lugar en la formación del mismo y las características necesarias para disponer de un mortero imprimible en 3D. Además, se ha realizado una revisión sobre la composición, morfología y microestructura de la concha de mejillón, así como experimentos previos relacionados con la introducción de la concha de mejillón en los materiales de construcción.

El diseño y la preparación de una serie de mezclas de i) mortero convencional y ii) mortero que incorpora concha de mejillón como agregado, formaron parte del trabajo experimental. Se llevó a cabo la caracterización de la concha de mejillón utilizada en estas mezclas y, finalmente, se realizaron diferentes ensayos mecánicos comparando ambos tipos de mortero.

Comparando los morteros preparados, convencionales y con concha de mejillón, se concluye que ambos presentan un comportamiento similar para la impresión 3D. Por lo tanto, la concha de mejillón puede ser utilizada en futuros experimentos de impresión 3D de morteros, aunque la presencia de materia orgánica y la forma de las partículas de la concha de mejillón hacen que el mortero tenga una fluidez y una resistencia en fresco ligeramente inferiores.

1.3 Resumo.

Este traballo céntrase no estudo dun tipo de material composto (composite), formado por morteiro e cuncha de mexillón (como agregado) na súa composición, co fin de investigar se cumpre os requisitos para ser imprimible en 3D mediante extrusión para o seu uso no campo da construción. A elección da cuncha de mexillón débese á gran cantidade deste tipo de residuos que se xeran en Galicia e que non se poden empregar facilmente para outras aplicacións.

Este traballo contén unha revisión bibliográfica de cada un dos compoñentes do morteiro, as reaccións que teñen lugar na súa formación e as características necesarias para ter un morteiro imprimible en 3D. Ademais, realizouse unha revisión da composición, morfoloxía e microestrutura da cuncha de mexillón, así como experimentos previos relacionados coa introdución da cuncha de mexillón en materiais de construción.

O deseño e preparación dunha serie de mesturas de i) morteiro convencional e ii) morteiro que incorpora cuncha de mexillón como agregado, formou parte do traballo experimental. Realizouse a caracterización da cuncha de mexillón empregada nestas mesturas e, finalmente, realizáronse diferentes ensaios mecánicos comparando ambos tipos de morteiros.

Comparando os morteiros preparados (os morteiros convencionais e os morteiros que incorporan cuncha de mexillón), conclúese que ambos presentan un comportamento similar para a impresión 3D. Polo tanto, a cuncha de mexillón pódese usar en futuros experimentos con morteiros para impresión 3D, aínda que a presenza de materia orgánica e a forma das partículas de cuncha de mexillón fan que este morteiro teña unha fluidez e unha resistencia en fresco lixeiramente inferiores.

2. Introduction.

2.1 Concrete, mortar and cement.

Both concrete and mortar are considered composites. Composites are composed by two or more individual materials (metals, ceramics and polymers). The goals of composites are the achievement of a combination of properties that are not present in any single material and the incorporation of the best characteristics of each of the component materials. Concrete and mortar are mainly composed by cement (the matrix), aggregate (the particulates) and water. Besides, supplementary cementitious materials can be added. In concrete, the aggregate is formed by sand and gravel meanwhile in mortar is just sand.[1]

Cement is a ceramic material finely powdered. In this powder, the shape of the particles is irregular (*Figure 1)*.

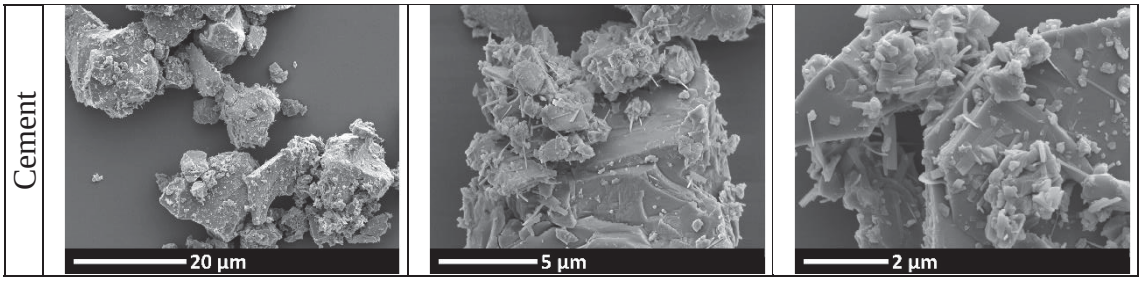

Figure 1. Scanning electron microscopy images of cement.

Cement is formed by clinker (described in the next section), gypsum, additives and additions. Gypsum is dihydrate calcium sulphate ($CaSO_4.2H_2O$). Additives can be natural inorganic mineral materials or inorganic mineral materials derived from the fabrication process of clinker and they are minority components in cement.[2] Exist a wide diversity of additions but the most common ones are blast furnace's slag, silica fume, limestone, fly ash, pozzolan and calcined schist.

In Europe, common cements are classified from types I to V depending on the mass percentage of clinker and additions in its composition. Cement I, denominated Portland cement and designed as CEMI, is the purest having between 95 and 100% in mass of clinker leaving the rest for additives, if any.[2]

2.1.1. Clinker of Portland cement.

The clinker is obtained from the sintering of a mix (crude) constituted by limestone and clay as prime matters. The crude must be finely divided and properly mixed in order to obtain a homogeneous product. The process of sintering consists in firing the crude in a kiln at a temperature range between 1350-1450˚C. The clinker of Portland cement is formed by 4 oxides, combined forming 4 "minerals" (*Table I)*:

Name	Brief formula	Composition	Mineral´s name	Mass percentage
Tricalcium silicate	C_3S	$3CaO\text{-}SiO_2$	Alite	35-70%
Dicalcium silicate	C_2S	$2CaO\text{-}SiO_2$	Belite	10-32%
Tricalcium aluminate	C_3A	$3CaO\text{-}Al_2O_3$	Celite	0-15%
Tetracalcium alumino ferrite	C_4AF	$4CaO\text{-}Al_2O_3\text{-}Fe_2O_3$	Felite	5-20%

Table I. Portland cement clinker's composition.[3]

2.1.2 Hydration of Portland cement.

Portland cement is a hydraulic conglomerate, that means, when the different components that form the clinker are mixed with water, exothermic hydration reactions take place. When these hydration reactions occur, the result is the setting of the mortar. The different hydration reactions are:[3]

- Hydration reaction of belite (C_2S):

$$2(2CaO{\cdot}SiO_2) + 4H_2O \rightarrow 2SiO_2{\cdot}3CaO{\cdot}3H_2O + Ca(OH)_2$$

By this reaction the products obtained are gel of tobermorite ($2SiO_2{\cdot}3CaO{\cdot}3H_2O$), (which is the responsible of the mortar's durability), and portlandite ($Ca(OH)_2$) (its basic pH, around 13, protects it from corrosion).

- Hydration reaction of alite (C_3S):

$$2(3CaO{\cdot}SiO_2) + 6H_2O \rightarrow 2SiO_2{\cdot}3CaO{\cdot}3H_2O + 3Ca(OH)_2$$

The obtained products are the same as in the belite reaction: tobermorite and portlandite.

- Hydration reaction of celite (C_3A):

Tricalcium aluminate gets hydrated very fast so at the time of making cement, it would set instantly. For that reason, to slow down the setting it is necessary to add gypsum ($CaSO_4.2H_2O$).

$$3CaO{\cdot}Al_2O_3 + 3(CaSO_4{\cdot}2H_2O) + 26H_2O \rightarrow 3CaO{\cdot}Al_2O_3{\cdot}3(CaSO_4){\cdot}32H_2O$$

Ettringite or Candlot's salt is the product from this reaction, and it has an expansive property because it considerably increases its volume.

- Hydration reaction of felite (C_4AF):

$$4CaO{\cdot}Al_2O_3{\cdot}Fe_2O_3 + 2Ca(OH)_2 + 10H_2O \rightarrow 3CaO{\cdot}Al_2O_3{\cdot}6H_2O +$$
$$3CaO{\cdot}Fe_2O_3{\cdot}6H_2O \rightarrow 6CaO{\cdot}Al_2O_3{\cdot}Fe_2O_3{\cdot}12H_2O$$

Portlandite ($Ca(OH)_2$) takes part in the reaction besides water and it is obtained hydrated calcium alumino ferrite, which is the responsible of cement's colour.

2.1.3 Supplementary cementitious materials.

In some cases, supplementary cementitious materials are introduced in the cementitious mix to improve determined characteristics as durability or resistance in mortar. Some commonly used are fly ash (FA) and metakaolin (MK).

Fly ash is obtained by electrostatic or mechanic precipitation of powdery particles that are carried by the gaseous flows of ovens fuelled by pulverized carbon. Fly ash can have two different natures: siliceous or calcareous. The main difference in their composition is the mass percentage of calcium oxide (CaO). Siliceous fly ash must not have more than 10% in mass of CaO meanwhile calcareous fly ash must have more than 10% of CaO.[2]

The shape of the particles in the siliceous fly ash, in contrast to the cement, is hollow spherical *(Figure 2)*:

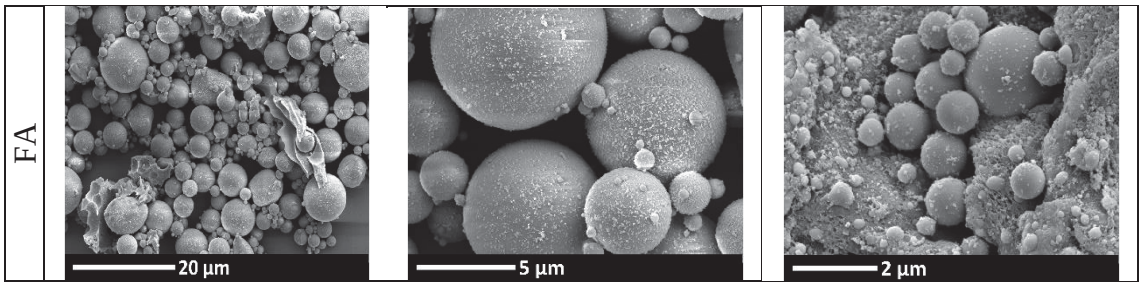

Figure 2. Scanning electron microscopy images of fly ash. Note Images provided by E.T.S.I de Caminos Canales y Puertos.*

Siliceous fly ash is a pozzolanic material. Pozzolanic materials do not set when they are mixed with water but when they are finely milled, at room temperature, they react with the dissolved calcium hydroxide ($Ca(OH)_2$), which is also called portlandite, and they form calcium silicon and calcium aluminate compounds that are able to develop resistance. The requirements in composition to be a pozzolanic material are that they need to be essentially formed by reactive silicon (SiO_2), which must be more than 25% in mass, and aluminium oxide (Al_2O_3). The rest of the material is composed by iron oxide (Fe_2O_3) and other oxides. The influence in the proportion of reactive calcium oxide (CaO) is insignificant in terms of resistance.[2]

Metakaolin (MK) differs from the rest of supplementary cementitious materials because it is not a waste product derived from industrial activities nor it is completely natural. MK is originated from the clay mineral called kaolinite and the obtention of this material comes from the calcination (thermal treatment), between a temperature range of 600 to 800˚C, of kaolin clays ($Al_2O_3.SiO_2.2H_2O$). By calcination, the water is driven off having as a result an amorphous aluminosilicate ($Al_2O_3.SiO_2$). The correct thermal treatment is important in order to obtain a highly pozzolanic material.[4]

The particles of metakaolin *(Figure 3)* are more fine and coarser that the cement ones, as the volume of the middle size particles is smaller.

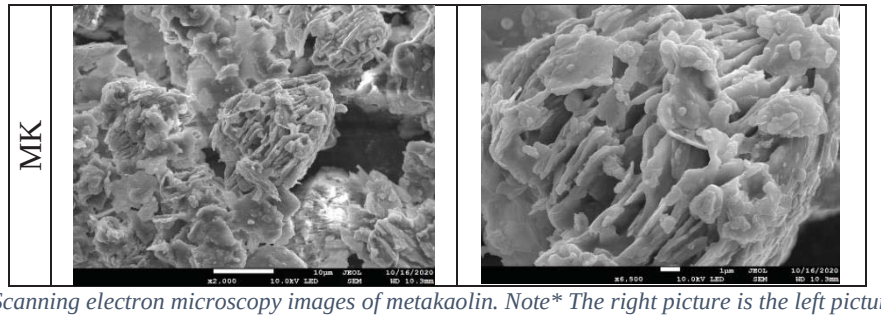

Figure 3. Scanning electron microscopy images of metakaolin. Note The right picture is the left picture zoomed. Images provided by E.T.S.I de Caminos, Canales y Puertos.*

2.2 Aggregate.

Conventional sand comes from crushing limestone, which is a sedimentary rock mainly composed by calcium carbonate in the crystalline form of calcite.

Recent studies incorporate mussel shell sand as aggregate in the fabrication of mortar due to its composition and shape of particles.[5–7] Mussel is a bivalve mollusc composed by two bluish black shells with tear shape, connected by a ligament in its dorsal part.[8] The shell can be divided in three parts: the external layer, periostracum, the medium layer called prismatic layer and the inner layer denominated nacre. The periostracum is formed by conchiolin (organic part), which is a combination of structural proteins.[9] The prismatic layer is formed by parallel calcite prisms and the nacre is composed by laminar aragonite.[8,10] Both calcite and aragonite are different crystalline forms (polymorphs) of calcium carbonate ($CaCO_3$). Vaterite, another polymorph of $CaCO_3$, is also present in the shell but is less stable and takes part on the shell's formation and development processes. The shape of the particles is very angular and sharp.[9,10]

Both aggregates are basically composed by calcium carbonate, differing in the presence of organic matter in mussel shell sand. Besides, the difference in shape between conventional sand and mussel shell sand (platelet sharp and much more angular in the case of mussel sand) will have a repercussion in mortar properties.

2.2.1 Galicia: source of aquaculture and its problems.

Galicia leads the aquaculture's production in Spain. Inside mussel's aquaculture, according to data in 2014, in Galicia 95.48% of global production is referred to mussel.[11] That is why Galicia counts with more than 3400 installations, which makes this autonomous community the most important one in the production of mussel in Spain.[12]

Due to this huge production a huge conserver industry has developed. Besides of being a big socioeconomic contribution, it generates residues which are the mussel's shells. As the shells constitute between 31 and 33% of the total weight of the mussel, more than 90.000 tons of residues are produced every year.[13]

Usually, the marine shells residues are used for fertilizer and bird's foodstuff. The problem is the morphology of mussel's shells, which present sharp sides that are harmful for birds. As a result, an important amount ends deposited in controlled landfills. For that

reason, it is important the investigation of its possible uses, as a brute material or as a source of new materials.

2.3 3D printing.

Three-dimensional printing is a revolutionary experimental technique where it can be created a wide variety of different three-dimensional structures based on a digital model performed by a specific software.

This technique can be applied to different fields:[14]

- Engineering and design: it gives the possibility of creating physical pieces that are difficult to acquire by price or that do not even exist in the market.
- Architecture: it lets the obtention of pieces used in construction or even in mock-ups. Big structures as houses or bridges can be constructed due to the great size scale in 3D printers.
- Domestic: printing small objects used in daily life is within almost everyone's grasp because of the reduced price in small basic 3D printers.
- Art: by using 3D printing, the obtention of unique pieces of art in terms of shape and size was achieved.
- Medical: this field has undergone a huge development up to the point of printing functional organs and prosthesis.
- Food: it is a curious field, since with this technology, it is possible to print edible foods with specific complex shapes.

Architecture stands out among the fields mentioned before because using 3D printing means a huge progress from the traditional construction techniques. Some of the most remarkable advantages are the elimination of moulds and formworks and the reduction of generated residues which are important due to the current environmental situation. Besides, the fabrication time and the workforce cost get considerably reduced.

In 3D printing, there are different techniques: material's solidification, injector's settle, extrusion and laminated.[14] Depending on the characteristics of the material that is going to be used to print, one or another technique will be chosen. Usually, 3D printing by extrusion is a common technique when the material used is mortar or concrete.

2.3.1 3D printing by extrusion.

3D printing by extrusion consists in extruding the material by layers, one over another, to form the required structure. To print by extrusion the mortar employed must have 4 critical characteristics:[15]

- Pumpability or flowability: refers to the reliability and ease with which the mortar is moved through the delivery system.
- Printability or extrudability: refers to the reliability and ease of depositing the mortar trough the deposition device.
- Buildability: it is the resistance of deposited wet mortar to the deformation under an applied load.
- Open time: it is the period where the properties above are consistent within acceptable tolerances.

The *Figure 4* summarizes all the information above, showing an example of proper values for viscosity and yield stress (open time) in order to have an optimum 3D mortar printing:

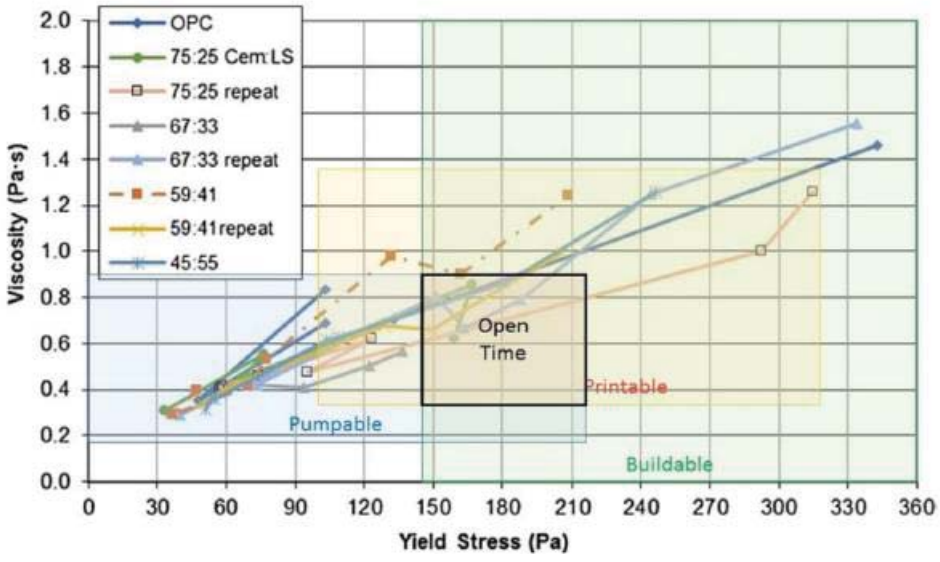

Figure 4. Schematic diagram showing the hypothetical parameters for 3D printable mortar. Note The legend refers to a set of cement pastes, with different ratios of ordinary cement and fine limestone powder.*[15]

The following table *(Table II)* shows the relationship between different mechanical tests that can be performed to study those mortar properties:

TEST	MORTAR PROPERTIES		
	Flowability	Extrudability	Buildability
Stress growth test	x	x	x
Flow curve test	x	x	x
Penetration	x		x
Shape retention			x
Open time			x
Green strength			x

Table II. Relationship between tests and mortar's characteristics in 3D printing.

As can be seen in the table above, most tests provide parameters for different mortar properties. These results permit stablishing relationships between them to lay down the values and ranges of use of mortar for 3D printing applications.

2.3.2 Rheology.

One of the most useful techniques to study the mechanical properties of 3D printing mortar is rheology. Besides, one of the most important mechanical properties to be considered is the thixotropy. Since both, rheology and thixotropy, are less known than other mechanical tests and properties to chemistry students, it is worth including a few words about them in this introduction.

Rheology encompasses the stress growth test (SGT) and flow curve test (FCT) of the previous table. Rheology is defined as the study of deformation and flow in materials. In the case of mortar, refers to the evaluation of yield stress (static and dynamic), plastic viscosity and thixotropy.[16]

The stress growth test, SGT, evaluates static yield stress. Static yield stress represents the stress necessary to initiate flow. Flow curve test, FCT, evaluates plastic viscosity and dynamic yield stress. Dynamic yield stress is the stress necessary to maintain flow meanwhile plastic viscosity expresses the resistance to flow, once the yield stress has been exceeded.[16]

Thixotropy is a reversible and time dependent process where the viscosity of a material, in this case mortar, decreases at a given shear rate. When mortar is at rest, its three-

dimensional network structure type develops over time. When applicating shear, the breakdown of this network structure is produced, and the reorientation or deformation of particles cause a reduction in its viscosity. When stop applying shear, the restructuration of the three-dimensional network occurs, and its viscosity is restored.[17]

When the extruding process in 3D printing, in the pumping phase a stress is applied, the thixotropy decreases and therefore a reversible reduction in viscosity takes place due to the restructuration of mortar's internal structure. In the "deposition", the thixotropy of the deposited (or extruded) phase increases, and consequently the viscosity does it too, being capable of setting and allowing the deposition of a new layer of mortar.[18,19] This process is clearly explained by *Figure 5*:

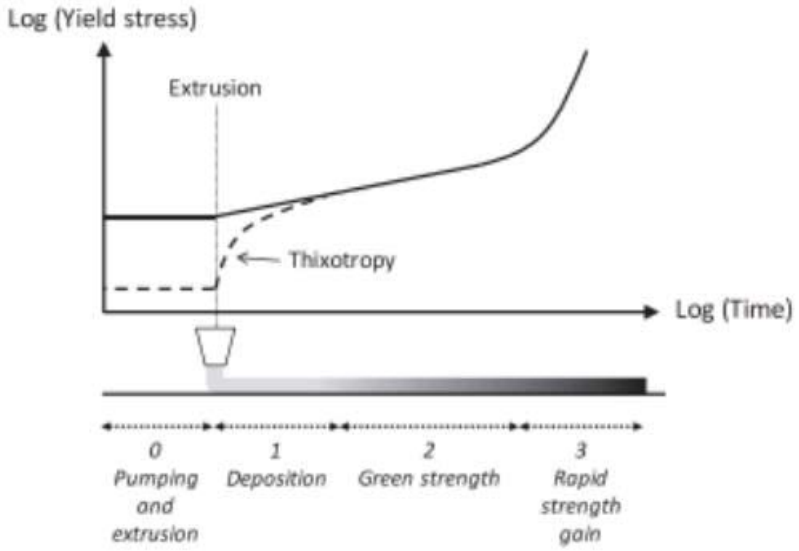

Figure 5. Evolution of yield stress with time during 3D printing extrusion of mortar.[19]

3. Objective.

Therefore, the **main objective** of this work is to analyze if mortar containing mussel shell sand as aggregate is valid to be used in 3D printing, as a solution to give the residues of mussel shells a second life.

The accomplish this objective, the preparation and characterization of mussel shell sand as well as the preparation of mortar mixes, with and without mussel shell sand, are required. By a series of mechanical tests, the necessary properties to have 3D pintable mortar are studied: flowability (rheological and penetration tests), extrudability (rheological tests) and buildability (rheological, penetration, shape retention, open time and green strength tests).

4.Experimental procedure.

The experimental procedure was carried out in two laboratories of the UDC: at the laboratory of QUIMOLMAT group in the CICA (Centro de Investigaciones Científicas Avanzadas), and at the laboratory of Ingeniería de la Construcción in Escuela Técnica Superior de Ingeniería de Caminos, Canales y Puertos.

Before the mortar fabrication, the characterization of both aggregates (conventional and mussel sand) was developed. During the granulometric analysis it was seen that they presented different particle size distribution, therefore, the first step carried out in the work was the correction of the size distribution of the conventional sand so that it presented a granulometric curve as similar as possible to the mussel shell sand.

Then, we perform several tests to compare the behaviour of two different types of mortars designed to be used in digital mortar: a conventional mortar using just conventional sand and a type of mortar that included mussel sand in its composition.

The tests carried out to characterize the mortars were the following ones: rheological test to define the very early age properties, shape retention, penetration test, open time, green strength and mechanical strength tests. Each of them will be described in detail along this part of the memory.

4.1 Preparation of samples of mussel shell.

The characterization of mussel shell was carried out in CICA (Centro de Investigaciones Científicas Avanzadas) so the preparation of the samples was required.

A previous grinded mussel shell (commercially available) containing particles with different sizes (some larger than 1 millimetre) was used for the preparation of the mixtures. Moreover, a preparation of the samples to be analysed was required. These analyses were carried out in the SAI (Servicio de Apoyo a la Investigación)

A sample of entire mussel shell was required to send to carry out scanning electron microscopy (SEM), which apparatus model was JEOL JSM-6400. Nevertheless, for X-Ray diffraction (XRD), X-Ray fluorescence (FRX), thermogravimetric and thermal differential analysis, it was necessary to grind the mussel shell sand in the laboratory, with a porcelain mortar, until its granulometry was up to 1 millimetre. The diffractometer

model used was Siemens D-5000 and the fluorescence spectrometer was S4 Pioneer BRUKER-NONIUS. The thermogravimetric and thermal differential analysis was made in a simultaneous analyzer TA Instruments SDT 2960 model.

4.2. Conventional sand's sieving.

As aforementioned, conventional and mussel shell sand presented different particle size distribution. To avoid the influence of these properties in mortar characteristics, the conventional sand was sieved to get the same grading curve as the mussel shell sand. To do this, it was necessary to get 270 kilograms of conventional sand and sieved it removing particles over 1 millimetre of diameter. This was done in an automatic sieve shaker model 105611 (*Figure 6).*

Figure 6. Automatic swinging sieve shaker.

In the sieve shaker, the recipient used had a capacity of about 1.5 kilograms. In *Figure 7* can be appreciated the result after sieved, having on the left the utile sand.

Figure 7. Sifted conventional sand.

Once the particles over 1 millimetre of diameter were removed, the granulometry of conventional sand and mussel shell sand, which already was 1 millimetre maximum, was performed. To do it, sieves of different opening were used: 0.5, 0.25, 0.125 and 0.063 millimetres. Three replicates of each aggregate were done.

4.3 Mixing procedure.

Before executing any test, it was necessary to mix the raw materials: conventional sand, cement, metakaolin, fly ash and mussel shell sand when required. The machine used was a Pan type mixer 56 litres capacity. Firstly, the conventional sand was mixed with the extra water (that was calculated to compensate the absorption at 10 min) for 1 min and then left to rest for another 9 min.

Then, cement along with the metakaolin and fly ash were added. After 1 min of mixing, water was introduced (80%). This powder-water contact is fixed as the reference time to develop the mortar tests. After 1 min of mixing, the remaining water was added. The mixing was continued for another 1 min, the mortar was left to rest for 5 min and finally mixed again for an additional time of 3 min.

For all mixes, the procedure was always the same *(Figure 8)* and the overall time was 22 minutes:

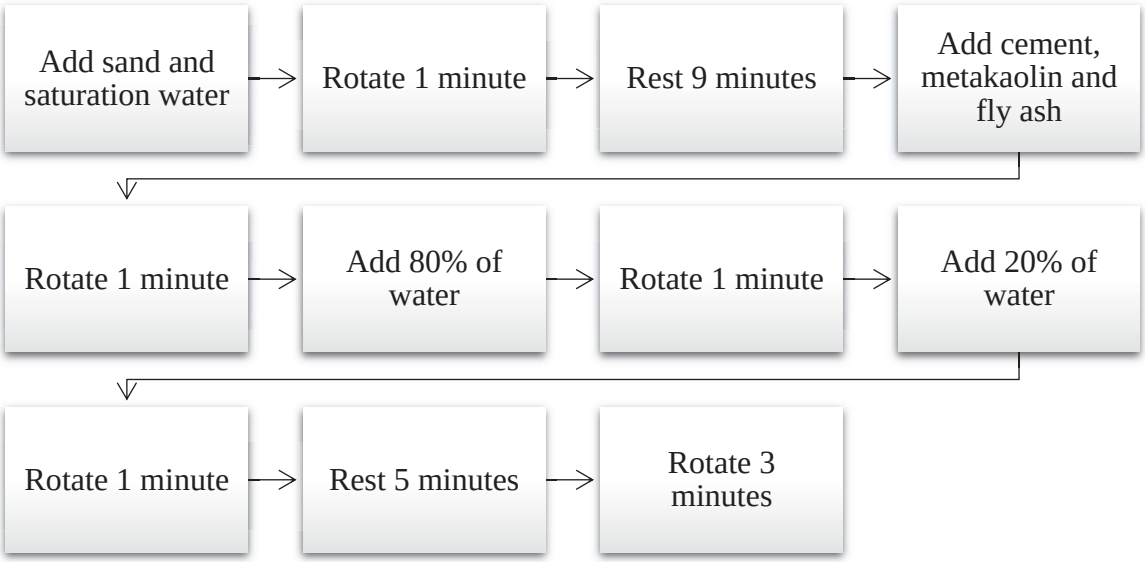

Figure 8. Mixing procedure.

In *Figure 9* can be appreciated the resulting mortar after mixing:

Figure 9. Fresh mortar resulting from kneaded.

Two mixes of each type of mortar were developed. From the first mix the material to carry out rheological, shape retention, open time and penetration tests was obtained. This mix was developed three times so that the tests can be replicated. From the second mix, the mortar used in green strength and mechanical strength tests was obtained. In this case, this mix was developed twice, to obtain two replicates of each type of test.

Depending on the group of tests, the quantities for each component of the mortar varied. For the first group of tests mentioned before, the total amount of mortar was 11 litres and

Table III shows the specific quantities for conventional mortar and mussel shell sand mortar:

	Conventional mortar	**Mussel shell sand mortar**
Material	Mass (g)	Mass (g)
Conventional sand	6608.3	3304.1
Metakaolin	1976.3	1976.3
Fly ash	3425.5	3425.5
Cement	4836.0	4836.0
Water	80%: 3720.0 20%: 930.0	80%: 3720.0 20%: 930.0
Saturation water	117.36	169.63
Mussel shell sand	-	3366.0

Table III. Quantities needed for 11l of mortar.

For the performance of green strength and mechanical strength tests the required amount of mortar had to be bigger, 28 litres specifically. Now, *Table IV* shows the quantities needed for each type of mortar:

	Conventional mortar	**Mussel shell sand mortar**
Material	Mass (g)	Mass (g)
Conventional sand	16821.0	8410.5
Metakaolin	5030.5	5030.5
Fly ash	8719.5	8719.5
Cement	12309.8	12309.8
Water	80%: 9469.12 20%: 2367.28	80%: 9469.12 20%: 2367.28
Saturation water	298.74	431.77
Mussel shell sand	-	8568.0

Table IV. Quantities needed for 28L of mortar.

In all tests, the measurements were taken at times 30, 45, 70, 105 and 150 minutes since the start of the mixing procedure. In terms of age, it would be 19, 34, 59, 94 and 139 minutes respectively, because age is started to be counted when the 80% of water is added to the mixer machine (water to cement contact).

4.4 Rheological tests.

The rheological behaviour of the mortars in fresh state was studied by performing a stress growth test (SGT) and a flow curve test (FCT). These two different tests were carried out

by using a Schleibinger Viskomat XL axial rheometer with a cone plate device, which inner diameter was 128 millimetres *(Figure 10)*.

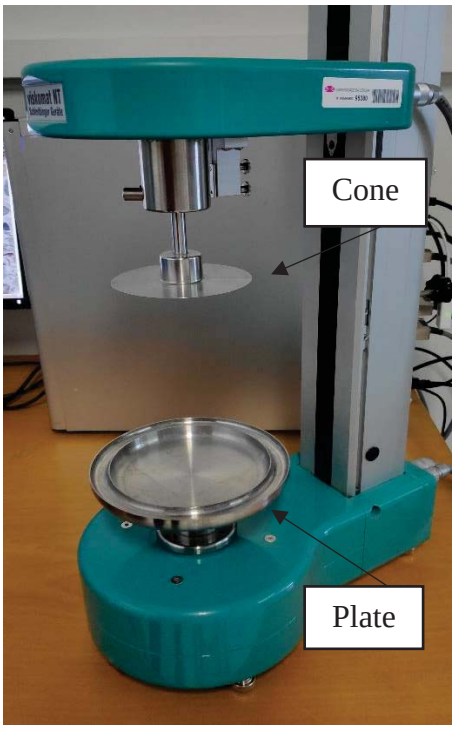

Figure 10. Rheometer.

Once the plate of the rheometer was filled up with mortar, the test could begin. The process of this test is reflected by the figure below *(Figure 11):*

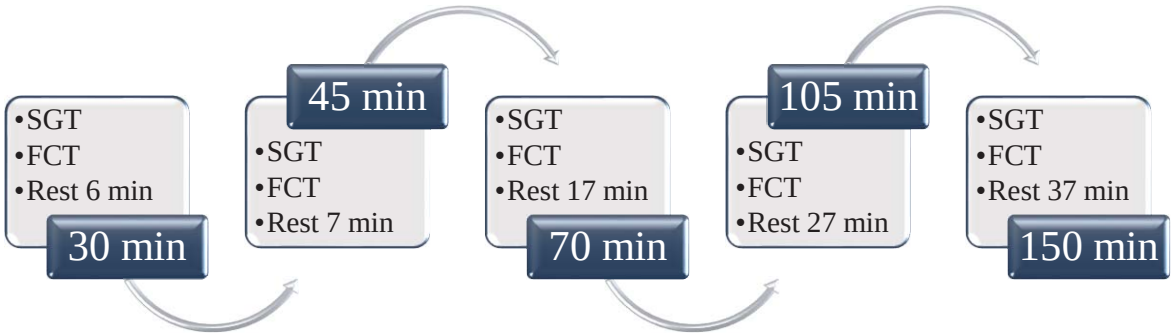

Figure 11. Rheological tests.

At each time, one SGT and then one FCT were done and between them, the mortar was manually stirred to avoid any orientation of the particles. First, the SGT consisted in submitting the mortar to a constant rotational speed of 6 rpm (revolutions per minute) for

60 seconds. The stress growth test is used to determine the static yield stress, which is defined as the stress needed to initiate the flow.

As a result of this test, a graph torque (N/m^2) vs time (s) was obtained, where the maximum corresponds to the static yield stress, *(Figure 12)*:

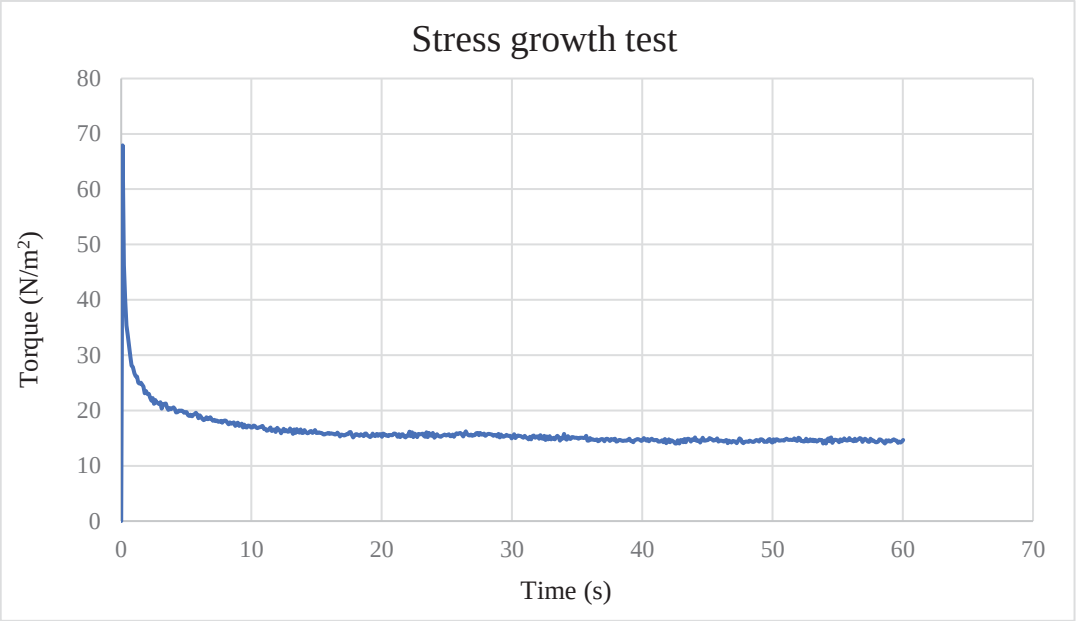

Figure 12. Stress growth test representation.

Then, the FCT consisted in submitting the mortar to different rotational speeds, from 119 to 0 rpm in intervals of 17 rpm. Each decreasing speed was applied for10 seconds, except the initial speed which was maintained for 40 seconds to achieve the structural breakdown of the mix, thereby avoiding the effects of thixotropy. The total time of the FCT was 105 seconds. This test allows to determine the dynamic yield stress and plastic viscosity.

This test gave a graph type torque (Nm) vs time (s), obtaining the torque pair associated at each step measured *(Figure 13)*.

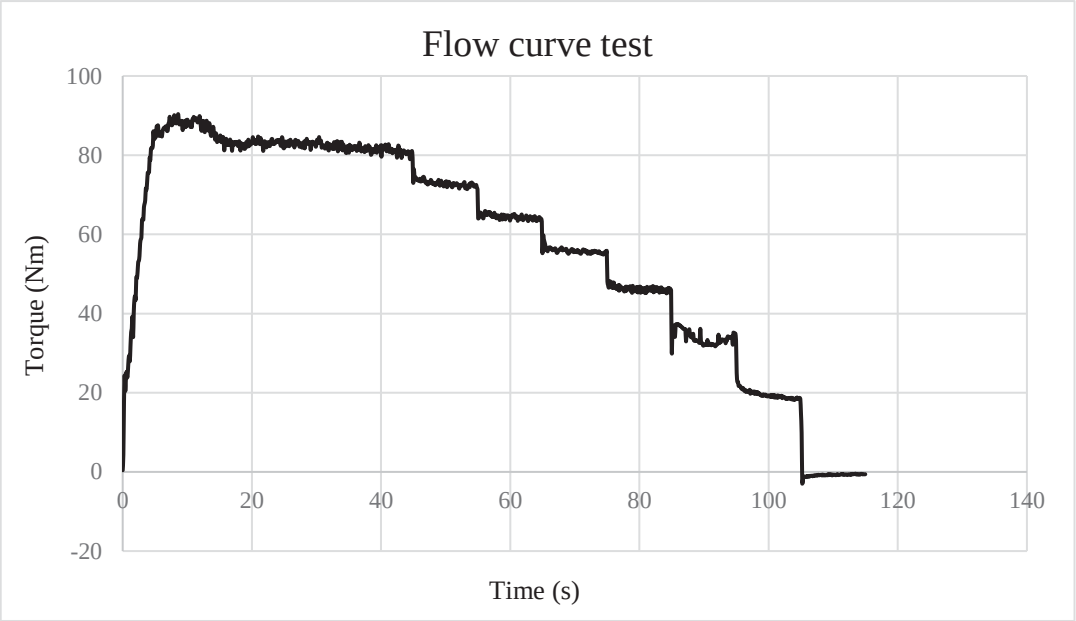

Figure 13. Torque vs time graph resulting from flow curve test (FCT)

4.5 Penetration tests.

The consistency of the mortar at the times stablished was measured performing the penetration test. A Plunger penetration apparatus E083 was used *(Figure 14):*

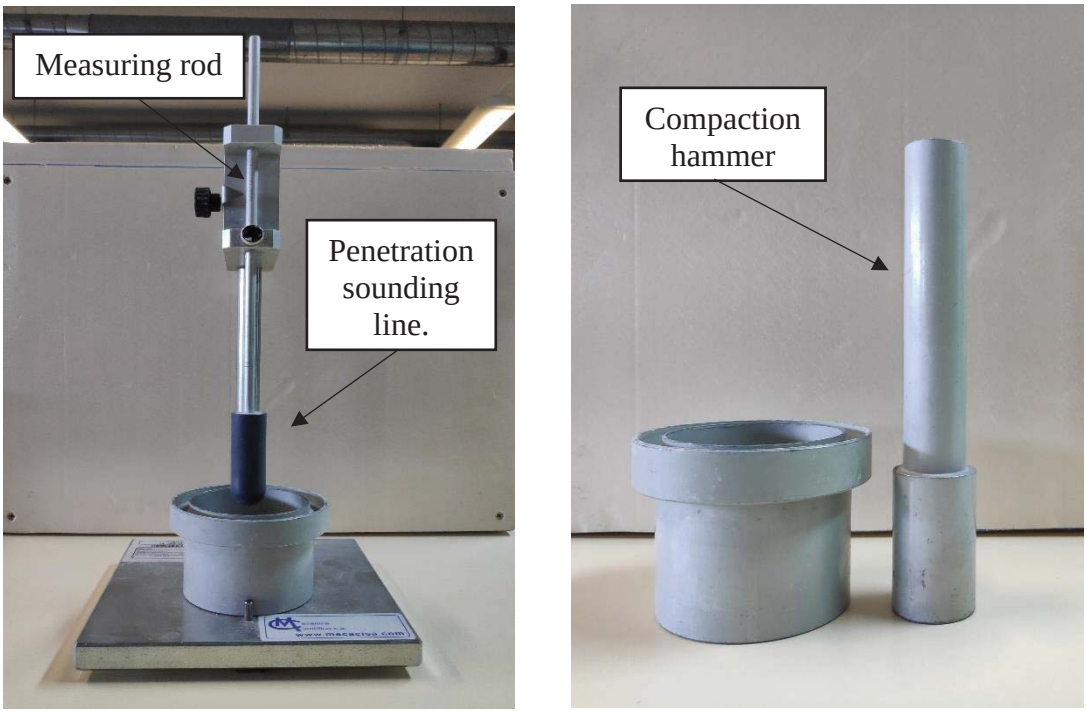

Figure 14. Apparatus used for penetration test.

The recipient, that presents an overflow's manifold, was filled up with mortar in two layers, compacting each layer applying 10 tiny hits using the compaction hammer. [20] Between each measurement, the surface must be flattened with the compaction hammer too. When the penetration sounding line fell free into the mortar, it made a hole on it *(Figure 15)* and the depth was looked it up at the measuring rod *(Figure 16)*.

Figure 15. Fresh mortar after open time test.

Figure 16. Measuring rod.

4.6 Open time tests.

For this test, it was used a Penetrometer EN13294 that incorporates a mould and a scale (precision ± 0.5 grams). First, the mould was filled up with fresh mortar in 10 steps, hitting each layer 4 times over the table. Then, it was levelled to the upper part of the mould using a rule. [21] The mould was covered with a tap with holes, where the penetration sounding line was going to go through. Each hole was used for a time measurement *Figure 17.*

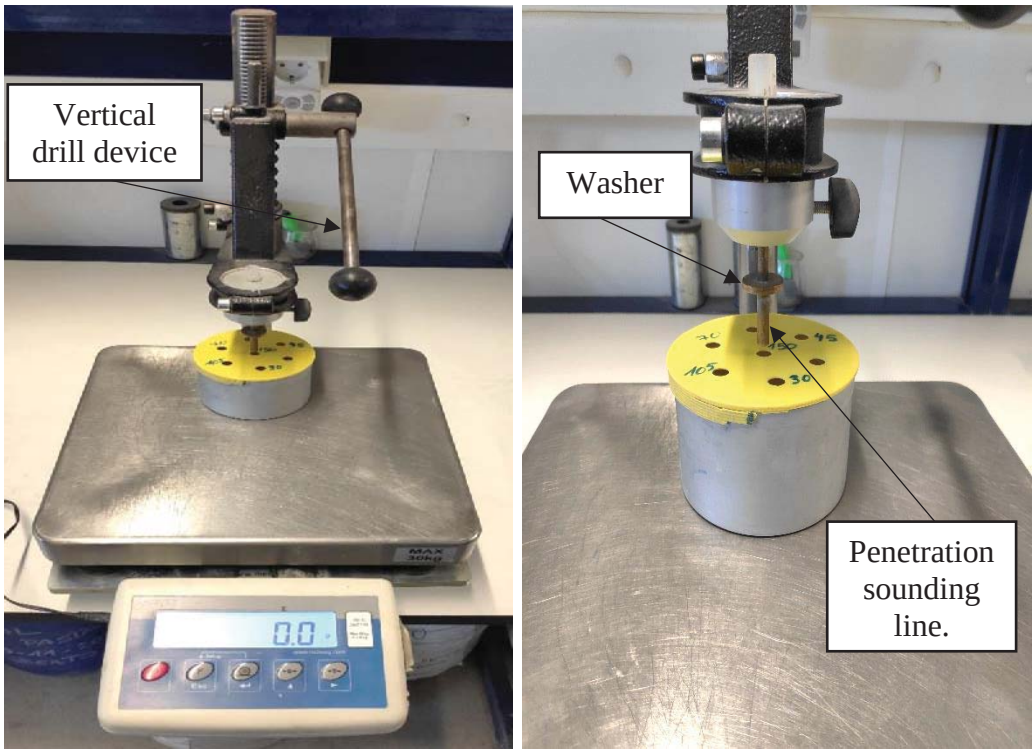

Figure 17. Open time test apparatus.

The full mould was collocated over the balance, and it was previously tared. Using the vertical drill device, the penetration sounding line went down in the sample until the washer brushed against the tap, which in this case was 2.5 centimetres. The indicated value on the balance, in grams, was noted down. The result of this test can be seen in the image below *Figure 18.*

Figure 18. Fresh mortar after open time test.

4.7 Shape retention tests.

This test consisted in filling up with fresh mortar 5 moulds of dimensions 30 centimetres height and 15 centimetres of diameter (*Figure 19)*. However, in this test, the moulds were levelled at only 15 centimetres height. The moulds were filled in just after mixing and then each mould was opened at different times (30, 45, 70, 105 and 150 minutes).

Figure 19. Mould used for shape retention test.

The final purpose of this test was to measure the difference in diameter of the fresh mortar after the opening of the moulds. The results can be appreciated in the following image *(Figure 20).*

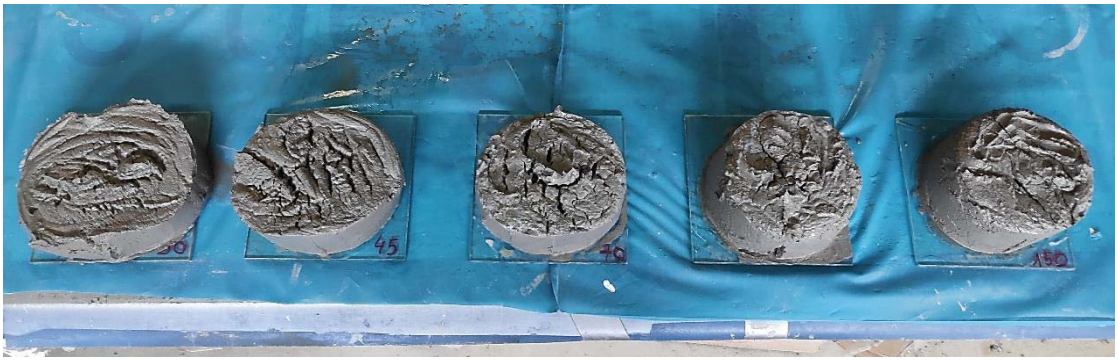

Figure 20. Fresh mortars after shape retention test.

The fresh mortars of the image are ordered in time increasing. The numerical measurements will be analysed in the *Results* part but just now looking at the image, it can be seen that the first two mortars have a considerably bigger diameter than the rest.

4.8 Green strength tests.

To perform this test, it was needed the 5 moulds used for the shape retention test *(Figure 19)* but in this case, the fresh mortar was levelled up to 20 centimetres height. The apparatus used was a Unitronic S205-05N which vertical cell load was 10 kN *(Figure 21)*.

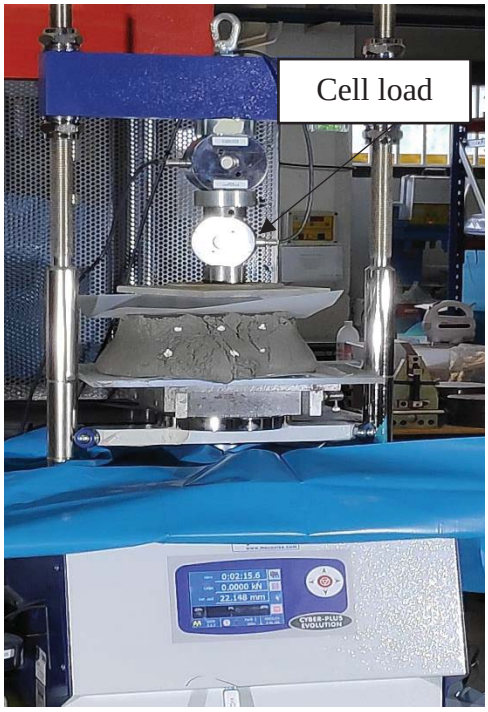

Figure 21. Green strength test apparatus.

Each test specimen was demoulded at the corresponding measuring time. Once demoulded them, over a methacrylate piece, it was measured the height and the diameter of mortar and then placed it in the apparatus. When the program began, the platform where the mortar was started to move up at a velocity of 25 mm/min, so we were registering once the test specimen made contact with the uniaxial compressive load. The displacement was the same length (12.5 centimetres) for all mortars, but as the initial height of mortar specimens was different depending on the demoulding time (increasing as time passed), the displacement length once the mortar contacted the load was different.

As a result, the maximum value of load registered was at a different maximum displacement length depending on the test specimen. After that, the mortar was taken off from the apparatus and the diameter and height were measured again.

4.9 Mechanical strength and density tests.

At the time of doing the green strength test, the initial step of mechanical strength tests was carried out too. This first step consisted in filling up with fresh mortar 10 moulds. Each mould had the capacity of three test specimens in the shape of quadrangular prism which dimensions were 4x4x16 centimetres *(Figure 22).*

Figure 22. Moulds for breaking test.

First, the 10 moulds needed to be weighted empty. Then, as with every test done before, each pair of them were filled up at the times stablished but following a specific procedure. At time 30 minutes, the respective 2 moulds were filled. However, the rest were filled up in two layers. The first layer was put on at time 30 minutes and then the second one was applied at the respective times: 45, 70, 105 and 150 minutes *(Figure 23)*. The moulds were weighted again full. The purpose of weighting the moulds before and after filling them was to calculate the density of fresh mortar.

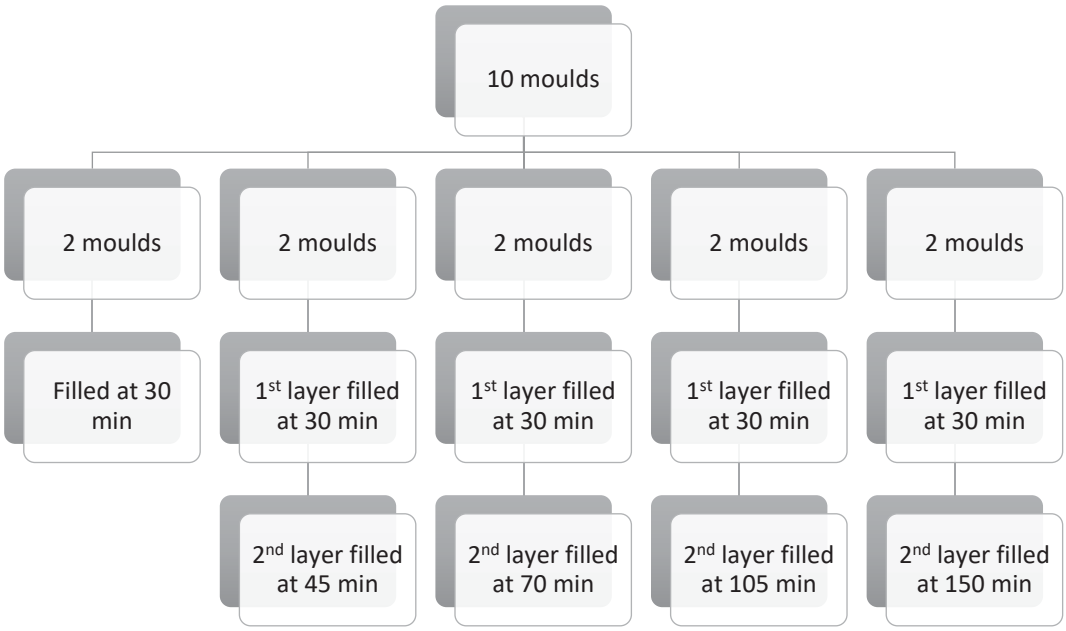

Figure 23. Moulds' filling procedure.

The moulds needed to be kept for one day, so they were put in a plastic bag, then closed and kept inside the climatic chamber. The next day, the test specimens were removed from their mould and the moulds were cleaned up because they were needed for the following replicate. Each test specimen was weighted individually and marked with a code on the levelled side. One example is *Figure 24*, that corresponds to 3 mortar test specimens (X, Y and Z) at time 30 minutes, replicate 1 with conventional sand (AM1) and mould M23. The objective of weighting them is to calculate the density of the mortar at age 1 day old.

Figure 24. Mortar test specimens at age 1 day old.

The curing process after one day (just after demoulding) was developed introducing the specimens in boxes filled up with tap water. This condition was necessary due to a phenomenon called shrinkage. Shrinkage is the process of losing the mixing water due to evaporation once the mortar is not in a 100% of relative humidity. This evaporation provokes internal tensions in the mortar that can originate reduction in its volume of even the failure. [22]

In the boxes, there were 6 mortar test specimens of each measuring time, having a total of 30, so 3 mortar test specimens of each measuring time would be used for mechanical strength test at 7 days and the other 3 of each were utilized for the tests at 28 days, that means, 15 mortar test specimens for each one of the days. The mechanical strength test consisted in two different tests: flexural and compressive strength test. First it was performed the flexural strength test and right after the compressive strength test.

Before starting the flexural strength test, it was necessary to take out the test specimens from the boxes and dry them with a wiper. Then, they were weighted to calculate, later, the density of mortar at age 7 or 28 days old.

The apparatus used for flexural strength test was the same for the green strength test *(Figure 21)* but including a flexion resistance breaking device. In one of the faces of the quadrangular prism was drawn two marks at 3 centimetres from each side. These marks indicated where the test specimen must be placed on the 2 support rollers *(Figure 25)*.

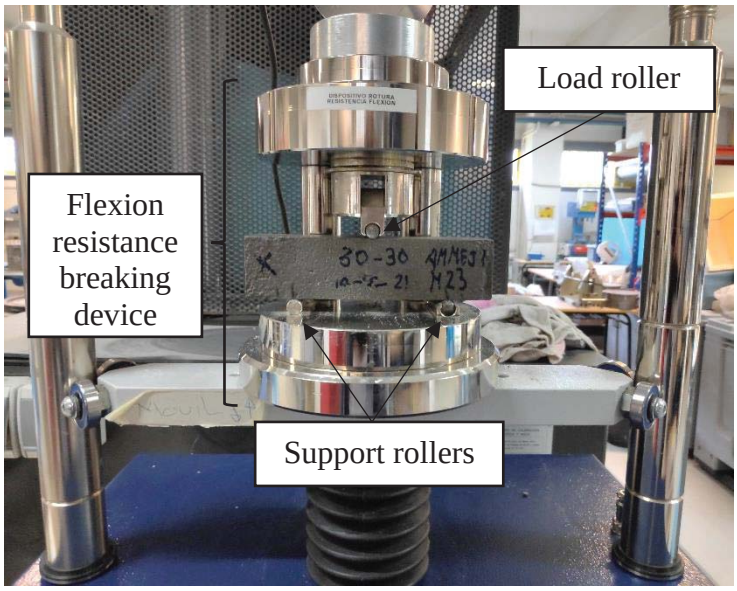

Figure 25. Flexural strength test apparatus.

In the image above, the mortar test specimen was collocated in the device perpendicular to the casting direction, following the standard, where the levelled face (where it is written the code) must be perpendicular to the load roller. In any case, this test was performed both ways, perpendicular and parallel to the casting direction. When it is parallel to the casting direction, not following the standard, the levelled side of the mortar prism had to be facing the load roller, it was the side where the load was going to be applied directly *(Figure 26).* [23]

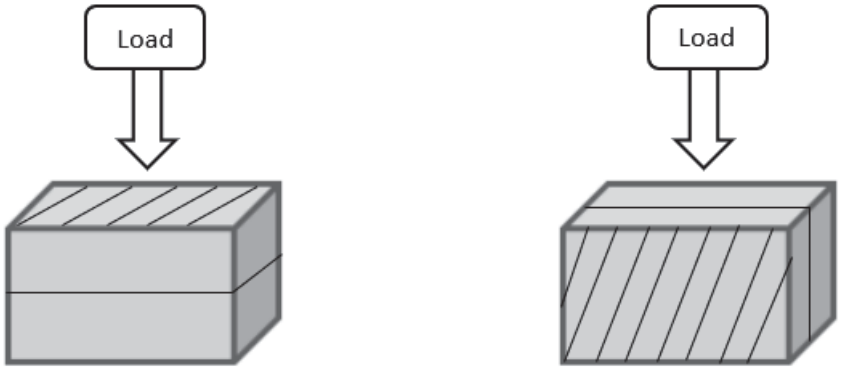

Figure 26. Representation of load applied parallel and perpendicular to the casting direction, respectively. Note The striped face corresponds to the levelled face.*

The scheme below *(Figure 27)* shows the mortar's test specimens distribution to perform the flexural strength test.

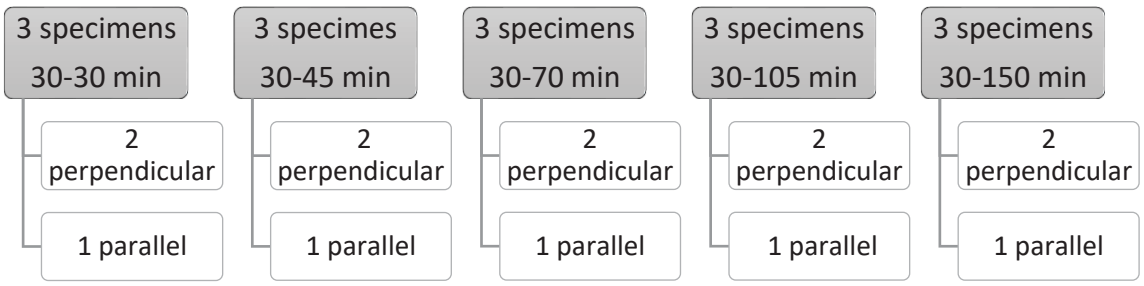

Figure 27. Mortar's test specimens distribution for flexural strength test.

As there were two replicates for this test, in the second replicate 1 test specimen was perpendicular to the casting direction meanwhile 2 were parallel for each time, to have as a result the same number of specimens perpendicular and parallel to the casting direction.

Once the test started, the applied load uniformly increased at a 5 kN/s until break. This test gave the breaking load and strength, and the reason of doing the test both ways, parallel and perpendicular, was to observe if there were any difference in these values.

The second part of the test was the compressive strength test and the test specimens used were the semi prisms resulting from the flexural test. To perform the test, the apparatus model used was an Ibertest PEV3005 *(Figure 28)*. In this case, the cell load was 60 kN for the conventional sand mortar and 300 kN for the mussel sand mortars.

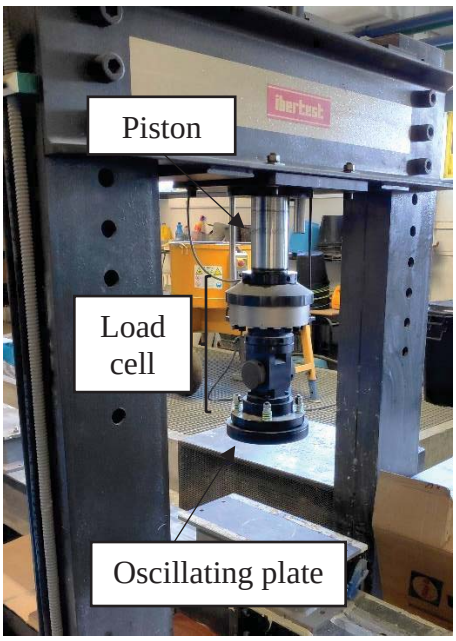

Figure 28. Compression test apparatus.

This test was done in the two ways (parallel and perpendicular) as in the flexural test. The parallel specimens used in flexural test were used then for parallel compressive test and the perpendicular ones in flexural for perpendicular compressive test. Thus, there was a mortar's test specimens specific distribution to perform the compressive test, which is shown in the scheme below *(Figure 29):*

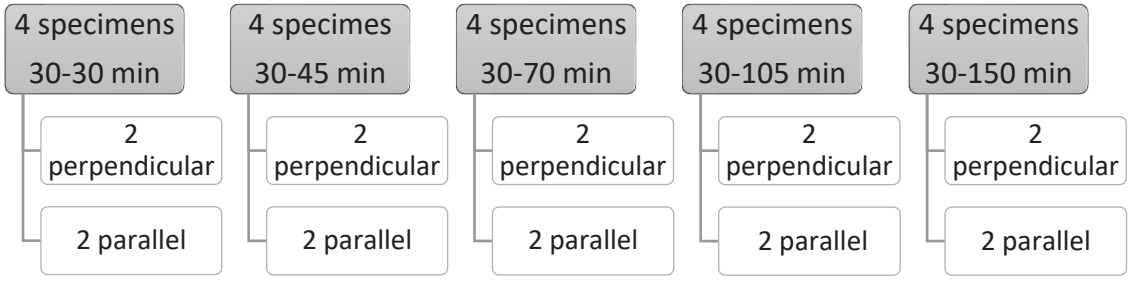

Figure 29. Mortar's test specimens distribution for compressive strength test.

In contrast to the flexural test, the specimens' distribution for the second replicate of the compressive test was the same as in the scheme above due to the pair number of specimens for each time measurement.

To collocate properly the semi prisms, a mark at 2 centimetres from the not broken side was drawn and right there, it was placed the semi prism in the device. After the compressive test, the resulting piece of mortar prism had to be a sand's clock shape. In *Figure 30*, it can be appreciated that the figure on the left was incorrectly broken meanwhile the right one has the correct shape.

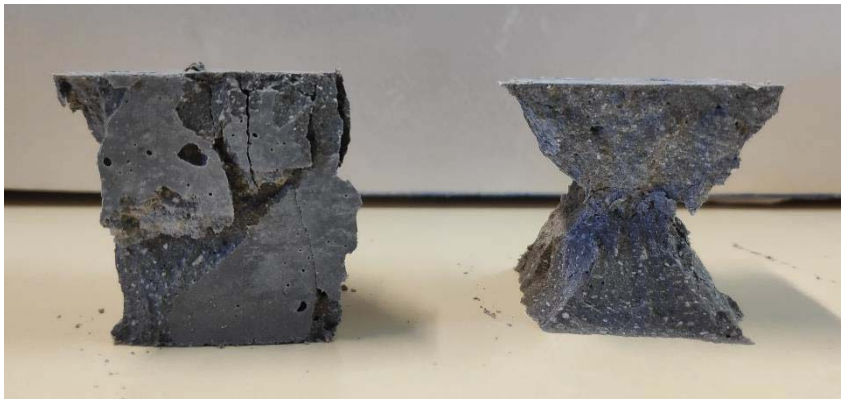

Figure 30. Pieces of mortar semi prisms after compression test.

5. Results and discussions.

5.1 Granulometry.

The granulometry of mussel shell sand and conventional sand are shown in *Figure 31*. It can be seen that both curves are similar although conventional sand contains more fine particles than mussel shell sand which can be influencing in some of the fresh state properties.

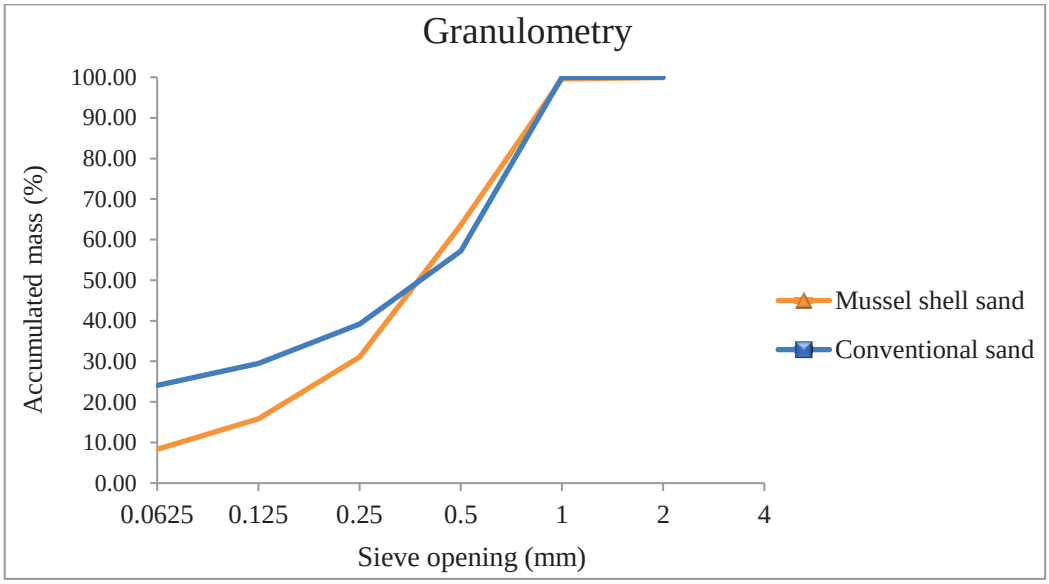

Figure 31. Granulometry of both aggregates.

5.2 Mussel's shell sand characterization.

By X-Ray diffraction (XRD), it was confirmed the presence of the three calcium carbonate polymorphs in mussel shell sand: calcite, aragonite and vaterite *(Figure 32)*:

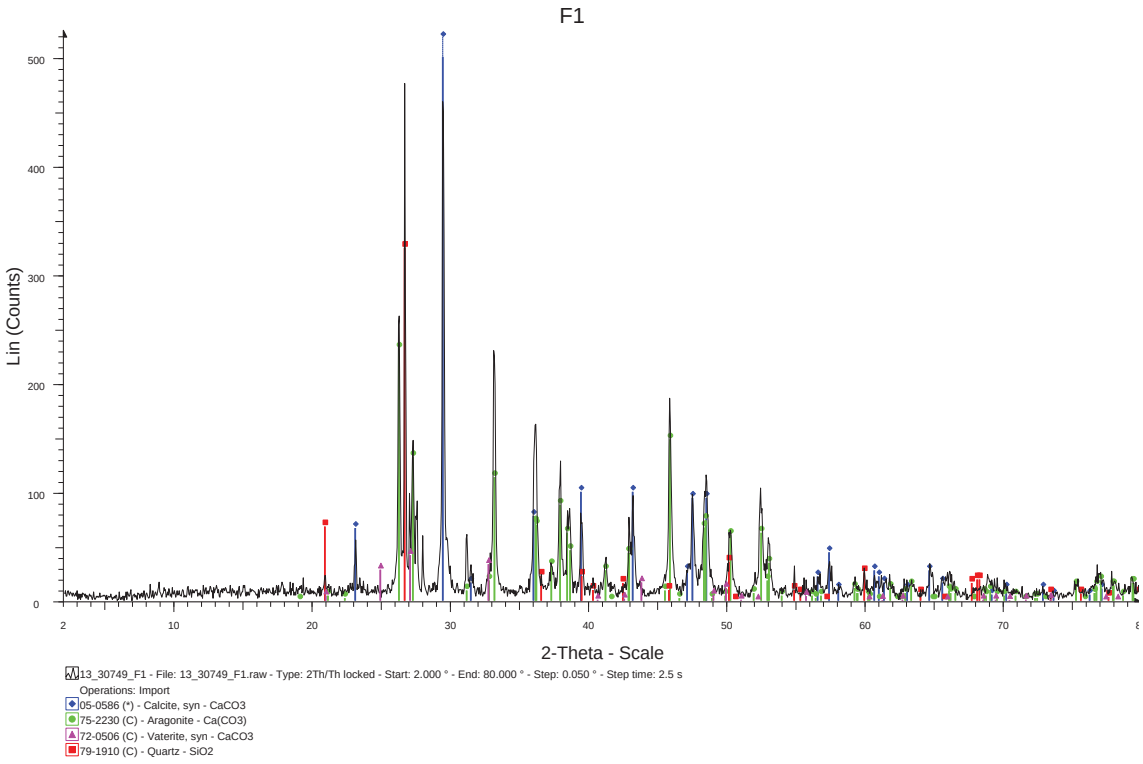

Figure 32. X-Ray diffraction of a mussel's sand sample.

Moreover, by scanning electron microscopy (SEM), it was verified the mussel shell´s microstructure *(Figure 33)*.

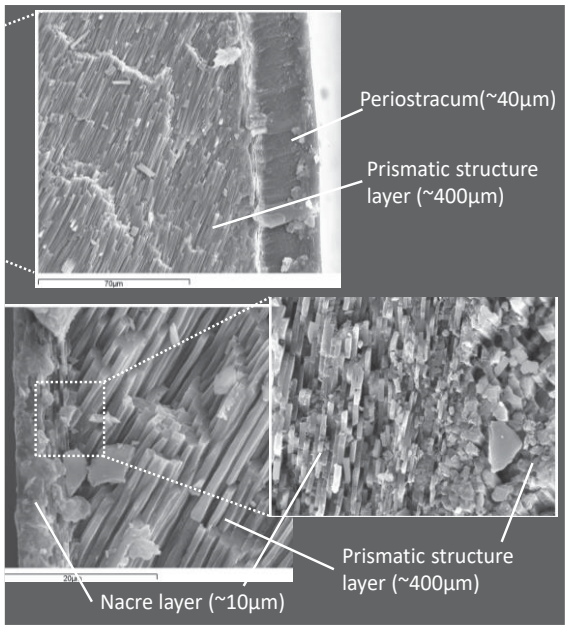

Figure 33. Description of mussel shell´s microstructure by SEM.

By X-Ray fluorescence (FRX) it was possible to know the composition of the mussel´s shell. To do it, five samples were characterized by this technique. The table below *(Table*

V) shows the results, where it can be observed that the principal compound in mussel´s shell is the calcium carbonate with a percentage of approximately 95%. The second compound is silicon oxide and the third one is sodium oxide, that can be associated to the presence of sodium chloride in the samples. The rest are present in a very low percentage.

Parameter	Mass percentage (%)
$CaCO_3$	94.664
SiO_2	2.580
Na_2O	0.508
Al_2O_3	<0.01
SO_3	0.308
MgO	0.277
Fe_2O_3	<0.005
SrO	0.192
K_2O	<0.006
P_2O_5	0.105
Cl	<0.009
Br	0.012
ZnO	<0.004
CuO	0.011
ZrO_2	0.010

Table V. Results of the majority compounds in mussel shell by FRX.

A thermogravimetric (green) and thermal differential (red) analysis were performed, and the results are shown in *Figure 34.* The continuous mass loss until 600˚C (about 7%) corresponds mostly to the loss of organic matter. In the thermal differential there is a peak at 285.5˚C which corresponds to an endothermic reaction due to specific organic compounds when their sublimation points are reached. From 600 to 800˚C there is an abrupt drop in the mass percentage, which is more than 40%. Furthermore, a new loss of about 1.2% occurs between 800 and 900˚C. These two are due to the decomposition of $CaCO_3$, emitting carbon dioxide (CO_2) and remaining calcium oxide (CaO) as a residue. Both peaks at 720.9 and 837.4 ˚C are endothermic reactions due to the decomposition of $CaCO_3$.

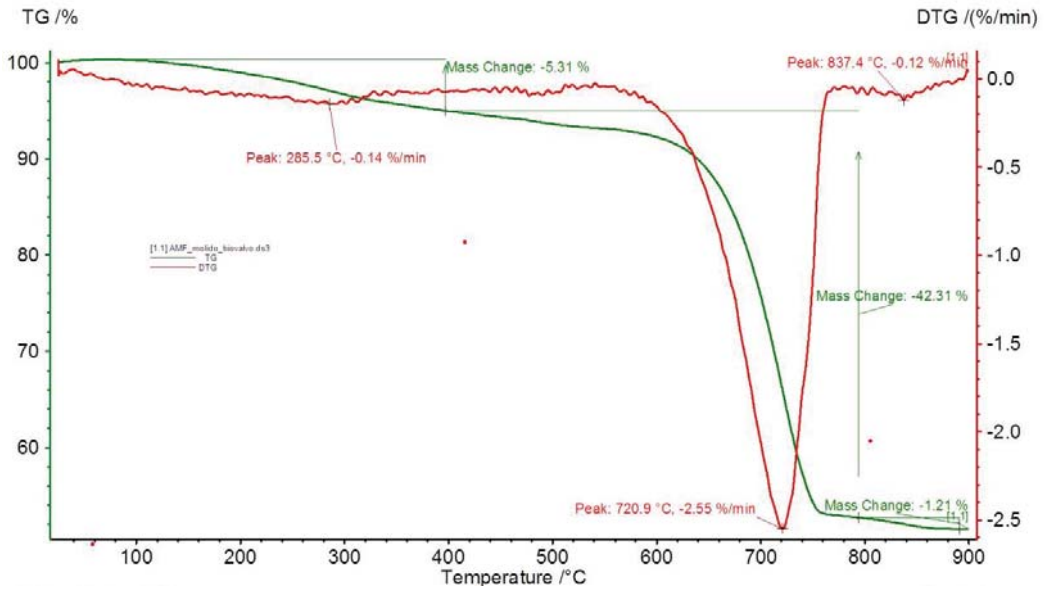

Figure 34. Results from thermogravimetric and thermal differential analysis.

5.3 Rheological tests.

Rheological tests can be divided in two tests: stress growth test (SGT) and flow curve test (FCT). SGT evaluates static yield stress meanwhile FCT evaluates plastic viscosity and dynamic yield stress.

5.3.1 Flow curve tests.

Figure 13 of the experimental procedure was transformed to fundamental units of shear stress and shear rate to give the so called flow curve. Rheology of mortar describes the Bingham model, which states that the relationship between shear rate and shear stress becomes linear once a certain yield stress has been passed. Its positive intercept refers to the dynamic yield stress meanwhile the slope corresponds to the plastic viscosity *(Figure 35)*.

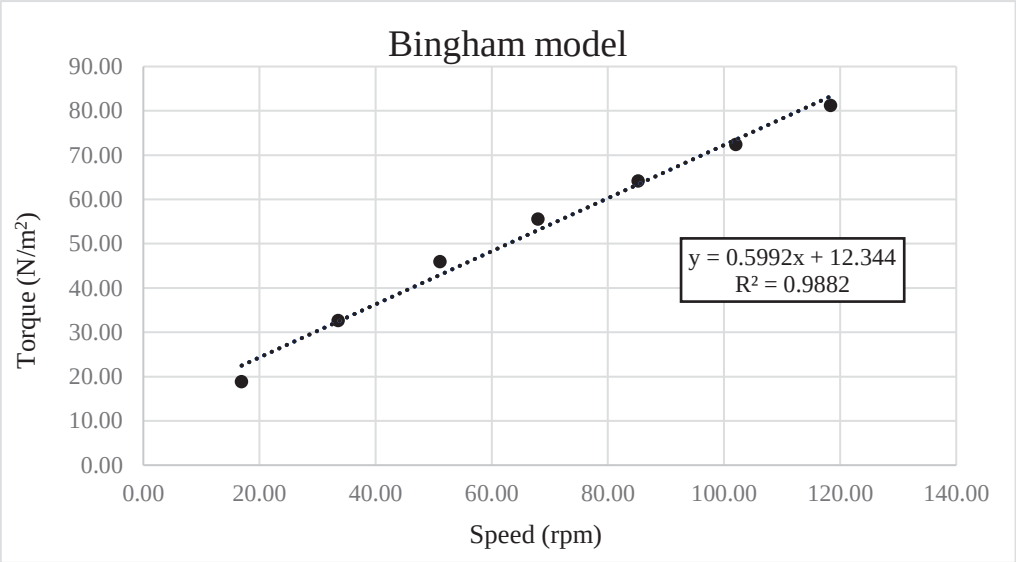

Figure 35. Example of Bingham model.

Then, with the experimental data obtained, two different plots were made in order to compare the dynamic yield stress and plastic viscosity of both types of mortar. In those graphics, and from now, **"AM" refers to conventional mortar meanwhile "AMMEJ" refers to the mortar with mussel shell sand too.**

For the dynamic yield stress plot, at the earlier ages, the dynamic yield stress is higher for the mortar with mussel sand as aggregate but then there is a change, having lower values than conventional mortar (*Figure 36).*

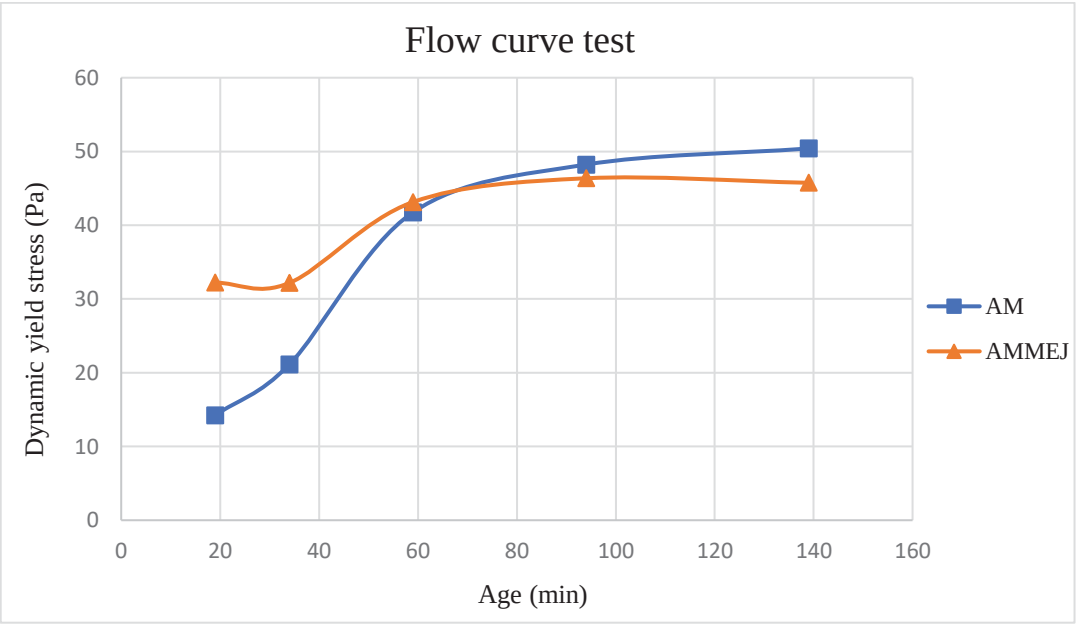

Figure 36. Experimental results for dynamic yield stress (FCT).

At earlier ages, the platelet shape of mussel sand makes the mortar more difficult to deform, which makes its dynamic yield to be higher in value than the conventional mortar one. Then, as the age increases, it takes part the hydration process. In conventional mortar, as the hydration reactions progress, the dynamic yield increases and therefore the difficulty to be deformed increases too. However, in mussel sand mortar, the presence of organic matter in mussel's particles affects the hydration process, retarding it, having as a result lower value in dynamic yield stress.

The experimental results for plastic viscosity are shown in *Figure 37*. It can be appreciated that the values of plastic viscosity for conventional mortar are higher than for mussel sand mortar at each of the measuring times and it hardly evolves with time.

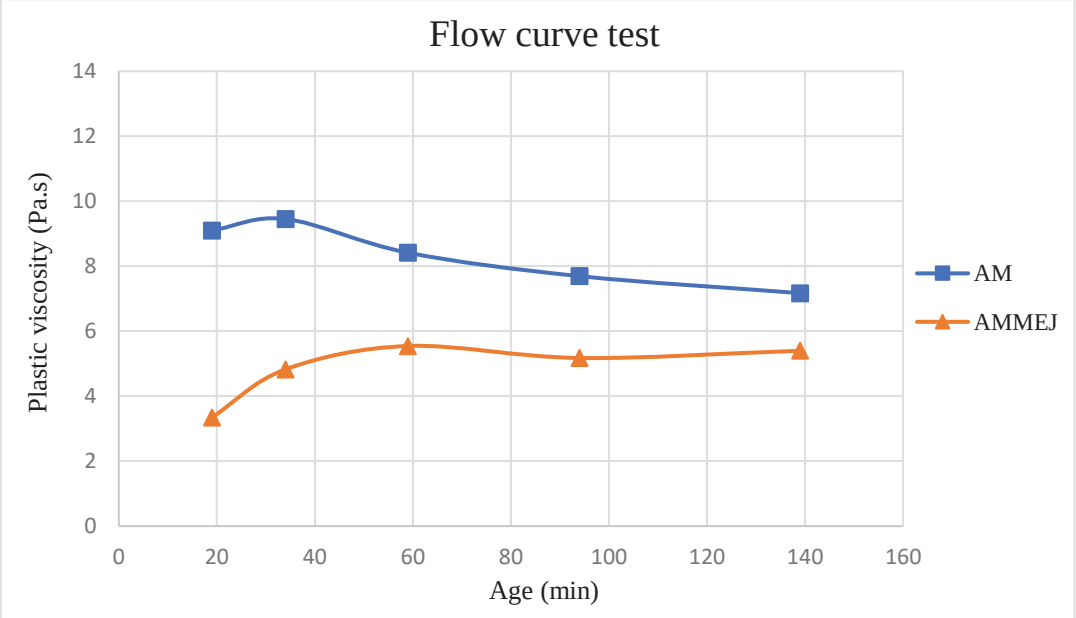

Figure 37. Experimental results for plastic viscosity (FCT).

Plastic viscosity is very related with the quantity of fine particles of the aggregate in the mortar. As the proportion of fine particles of aggregate increases, plastic viscosity does it too. When looking at 5.1 conclusions section, it can be appreciated that conventional sand owns more proportion of these fine particles than mussel shell sand, and consequently, its plastic viscosity is bigger.

5.3.2 Stress growth tests.

In order to compare the static yield stress for the two types of mortar, a plot was made, where each of the points at the ages stablished is the mean value of 3 values *(Figure 38)*.

Both types of mortars follow the same tendency, having similar values of static yield stress and similar evolution with time. It can be appreciated how at ages 19 (having 6 minutes rest), 34 (rest 7 minutes), 59 (rest 17 minutes) and 94 (rest 27 minutes) min old the static yield stress hardly increases while at age 139 min old (rest 37 minutes) suffers a visible increase.

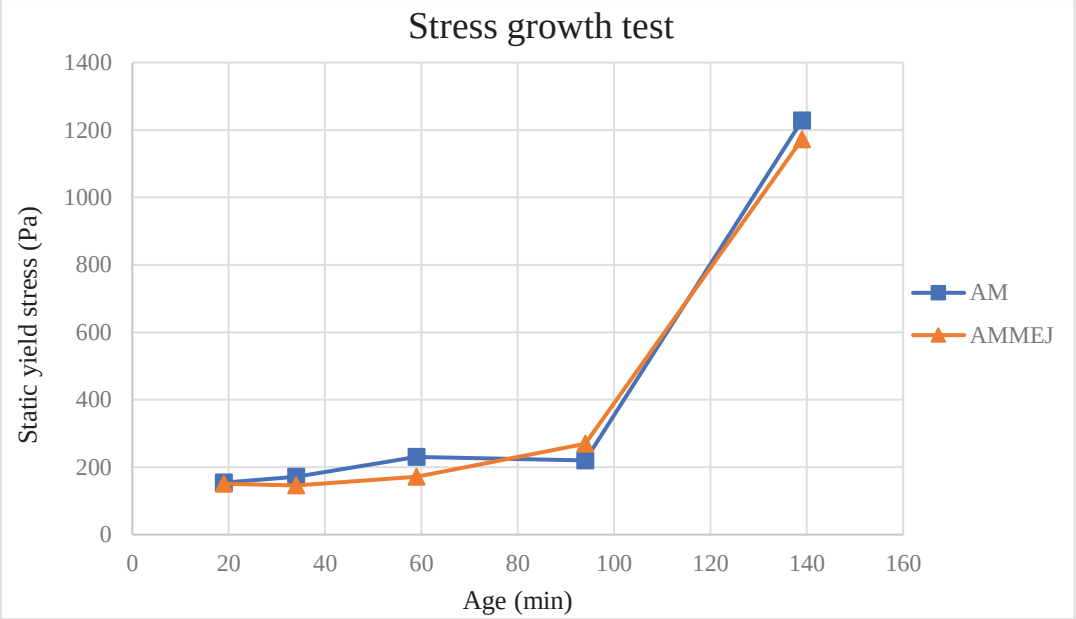

Figure 38. Experimental results for static yield stress (SGT).

When each one of the tests started, the deformation of fresh mortar's internal structure occurred and once the test stopped, it began the mortar's microstructure restructuration. The presence of mussel shell sand as aggregate makes more difficult the restructuration once the test stops so the mortar is easier to deform and therefore becomes easier initiate the flow too. However, this particle shape promotes interlocking, which counteracts this effect, leading finally, the mussel mortars to present a similar static yield stress as conventional mortars.

5.4 Penetration tests.

Based on the experimental data for both types of mortar, the results are reflected in the following graph (*Figure 39)*. Each plot has 5 points, which is the mean of 3 experimental values, referring to the different time measurements (19, 34, 59, 96 and 139 minutes old).

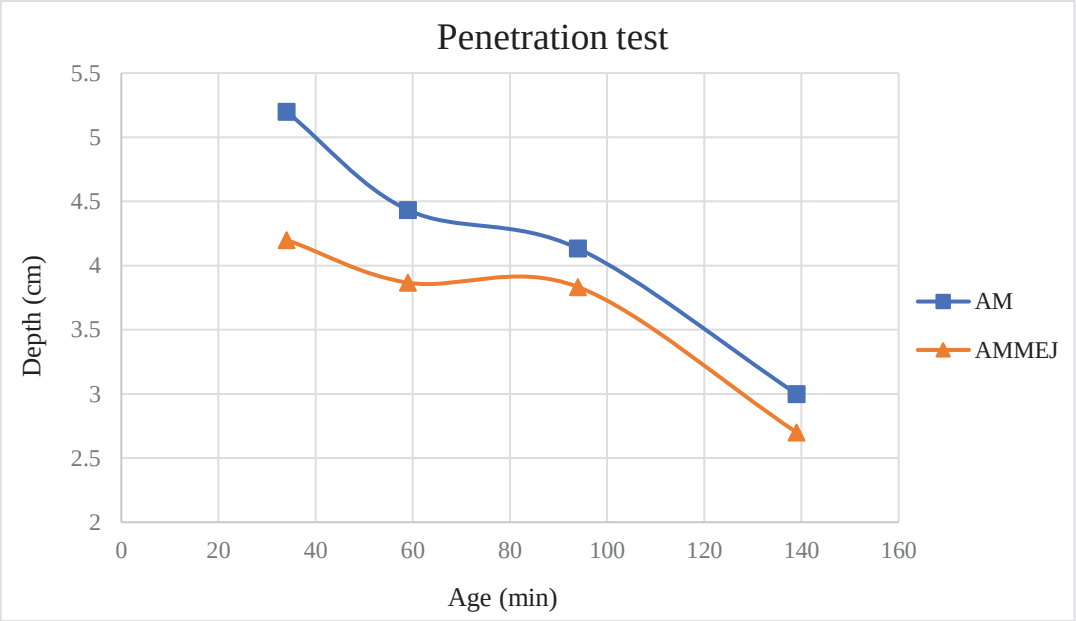

Figure 39. Experimental results for penetration test.

Both conventional and mussel mortar present higher values of consistency as the age increases (lower values in penetration depth), showing an evolution trend very similar. However, having the mortar with conventional sand exhibits always a higher penetration value than mussel mortar at each age. This test measures consistency but it is more sensitive than other methods to the particle shape as it assesses the opposition of the mortar to be penetrated by the penetrating probe. This justifies the differences between conventional and mussel mortar. Conventional sand is crushed but regular (all dimensions are similar) meanwhile mussel sand is irregular. When the penetration sounding line falls free into the mussel shell sand mortar, the mussel's platelet disposition creates an extra impediment when penetrating having as a result lower value in depth than the conventional mortar.

5.5 Open time tests.

Once again based on the experimental data obtained, the means where calculated, where each point of the plot is the mean of 3 experimental values *(Figure 40)*:

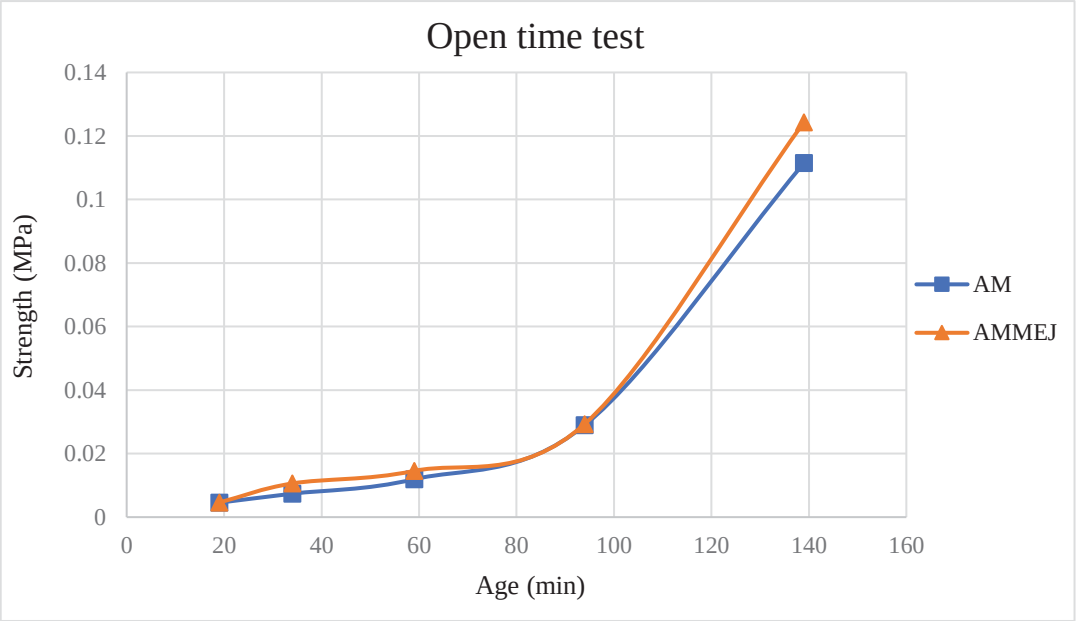

Figure 40. Experimental results for open time test.

In this case, again the values of strength increase with time in a similar way in conventional and mussel shell mortars. The particle shape of the sand is also influencing the results, but in this case, due to the test procedure and to the probe surface (smaller when compare with the one used in the penetration test), the differences between conventional and mussel shell mortar are slight.

5.6 Shape retention tests.

With the experimental data obtained, the shape retention factor (SRF) was calculated. The SRF is the relationship between the cross sectional area of mortar before demoulding, 15 centimetres, and the cross sectional area of mortar after demoulding. Again, the mean of each point of the plot is the average of three values. *Figure 41* shows the results:

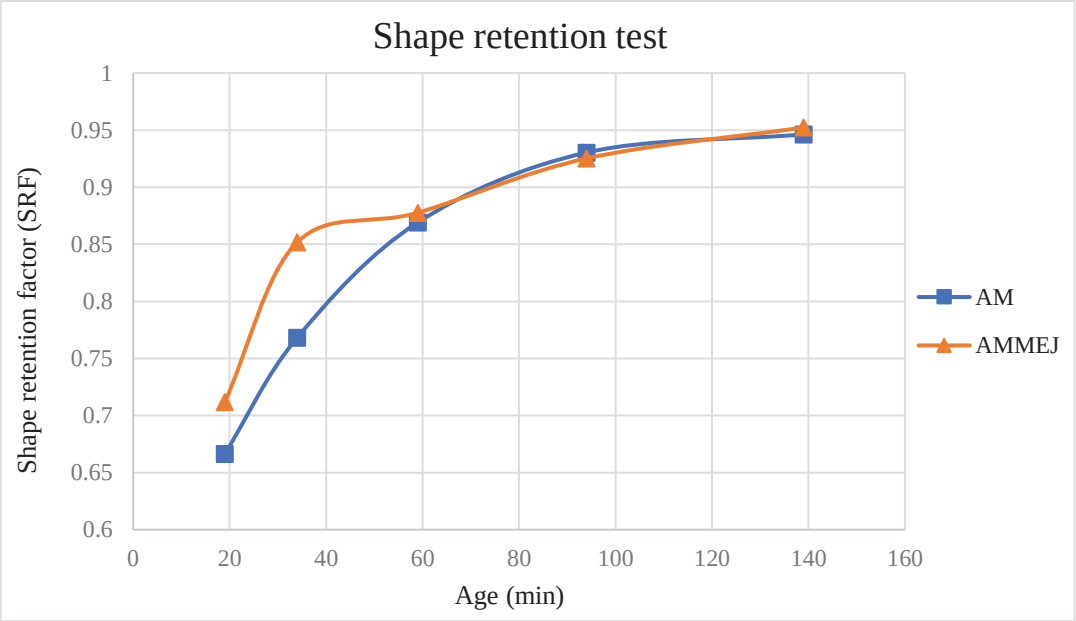

Figure 41. Experimental results for shape retention test.

Similar results were found for "AM" and "AMMEJ" mortars, only differing at 19 and 34 minutes old. At these ages, the use of mussel shells as aggregates leads to higher values in SRF.

This test is related to thixotropy and hydration. Mortars highly thixotropic are going to present higher shape retention factors. In addition, as the hydration takes place, the shape retention will be also higher. This effect can be seen in the graph where both mortars show higher shape retention values with age.

According to the stress growth test, both mortars present a similar thixotropic behaviour, therefore the differences at early ages are not due to this property. In addition, at early ages, both mussel and conventional mortar, are going to present similar and low hydration rate. Therefore, again, the particle shape of mussel sand is the origin of these differences. Particles are flaky and angular, which will promote their interlocking, increasing the value of the retention factor. As a result, and according to the measured values, the mussel mortars present higher retentions factors than the conventional mortars at early ages.

As the time goes by, due to the organic matter of the mussel shells, hydration of conventional mortars evolves faster than in mussel mortars leading conventional mortar to get similar values of shape retention than mussel mortar.

5.7 Green strength tests.

The mortar test specimens used in this test showed one or two types of failure patterns when a uniaxial compressive load is applied. For immature specimens (30 and 45 min old), the failure pattern was a significant lateral deformation under the action of an increasing load due to vertical displacement. This behaviour corresponds to a plastic and deformable type of material. However, mature specimens (70, 105 and 150 min old) presented less expansion in terms of lateral deformation but showed a shear crack pattern. The hydration reactions in these mortars led to develop structural rigidity so the tensile stress acted on the lateral deformation. Besides, the cohesion between particles was overtaken and shear planes appeared. This last pattern indicates the beginning of the setting process as well as the transition from the green to the compressive strength.

The images below *(Figure 42)* are a comparison for this test, where the first one corresponds to fresh mortar after demoulding meanwhile the second one belongs to the mortar after performing the green strength test, where it can be observed the shear cracks. These specific pictures are for mortar at the measuring time of 150 minutes.

Figure 42. Fresh mortars before and after performing green strength test.

In the table below *(Table VI)*, are shown the angles of the shear cracks for both types of mortar, conventional and mussel shell sand mortar, at mature ages (min old).

Mortar age (min)	70	105	150
Conventional mortar	50˚	60˚	60˚
Mussel shell sand mortar	50˚/55˚	50˚/55˚	60˚

Table VI. Resulting angles for shear planes.

As the age of mortars increases, the hydration reactions advance and therefore the structural rigidity increases, making the mortar resist larger load. This increase in load makes bigger angles when the cohesion between particles is surpassed.

Looking at the bibliography, the theoretical aspect of the plot after doing the green strength test is shown in *Figure 43*, where the legend refers to the ages when the mortars were tested.

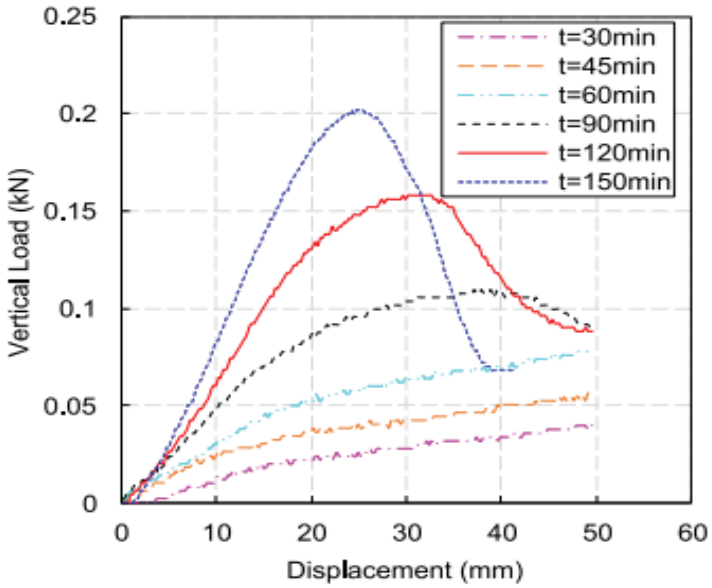

Figure 43. Green strength test for specimens of different ages. [24]

At the initial stage, the test specimens at early ages (30, 45 and 60 min old) followed a linear tendency of increasing load with vertical displacement. Then, they reached a large plateau in load even though the vertical displacement continued increasing. In the case of mature specimens (90, 120 and 150 min old), they also followed that linear tendency until reaching a peak value and then drop the load with vertical displacement due to the small stiffness of the specimens. [24]

The plots obtained in the laboratory just showed that linear tendency for all ages, due to the lack of vertical displacement in the apparatus. One example is *Figure 44*, where it is

shown the linearity of vertical load with displacement for a mortar test specimen of 105 minutes old.

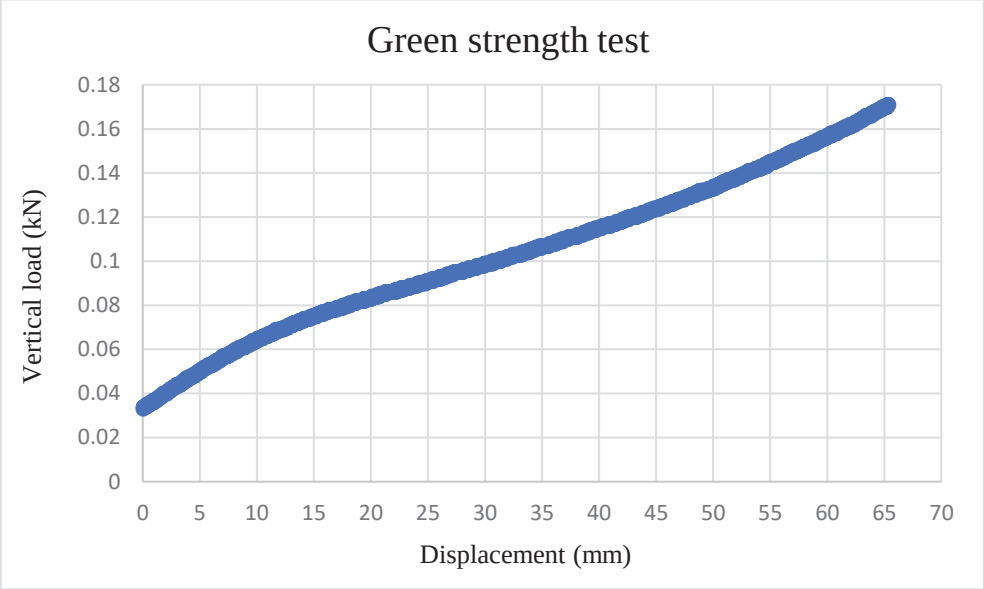

Figure 44. Green strength test for a 105 min old mortar specimen.

To compare the experimental results obtained for both types of mortar in this test, a plot maximum load versus age was made *(Figure 45)*. As it was previously said in the experimental procedure, the maximum displacement length depended on the age of the mortar. Thus, each of point for the same age are taken from the same maximum displacement.

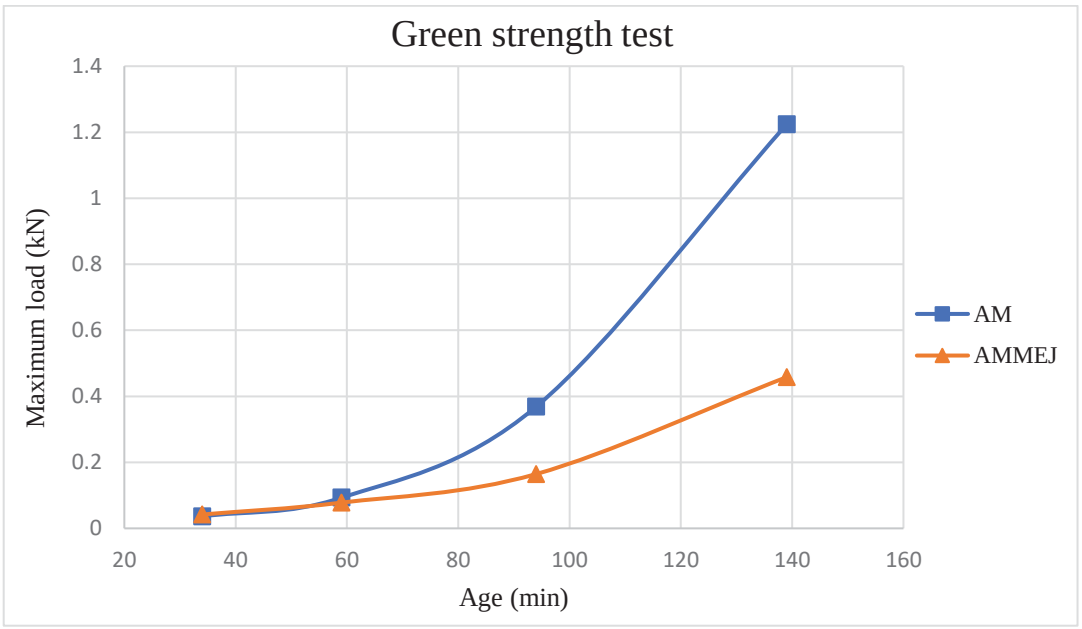

Figure 45. Experimental results for green strength test.

The results obtained are associated to two factors: hydration and adhesion. For early ages (34 and 59 minutes old), the values for maximum load are quite similar. However, at more mature ages (94 and 139 min old), the values of maximum load are bigger in conventional mortar than in mussel shell sand mortar. At these mature ages, the hydration reactions for conventional mortar are more advanced than for mussel mortar because the organic matter present in these kind of sand retards the process (same explanation that for dynamic yield stress). Besides, the use of mussel shell sand as aggregate makes a worse adhesion between the components of mortar due to its platelet shape, provoking less shape stability and therefore smaller value of load.

5.8 Mechanical strength tests.

Two different kinds of experimental data were obtained from mechanical tests: flexural strength and compressive strength. The objective is to compare each of them in terms of mortar's age (at 7 and 28 days old) and by the position they were collocated in the testing device (parallel or perpendicular to the casting direction), analysing the influence of the time between layers.

5.8.1 Flexural strength tests.

Based on experimental data, the means' values of the mixes with and without mussel shell sand were calculated. This test was performed at 7 and 28 days old in specimens filled at different ages: 19, 34, 59, 94 and 139 min old. In the following graph *(Figure 46)* is shown the experimental results for mortar perpendicular to the casting direction.

The experimental data for parallel orientation was not conclusive, it did not follow a clear tendency, probably due to the lack of data, so it was decided not to take into consideration in this work, so just the results for perpendicular orientation (according to the standard) are presented. The analysis of results under the other orientation could be a future line of investigation.

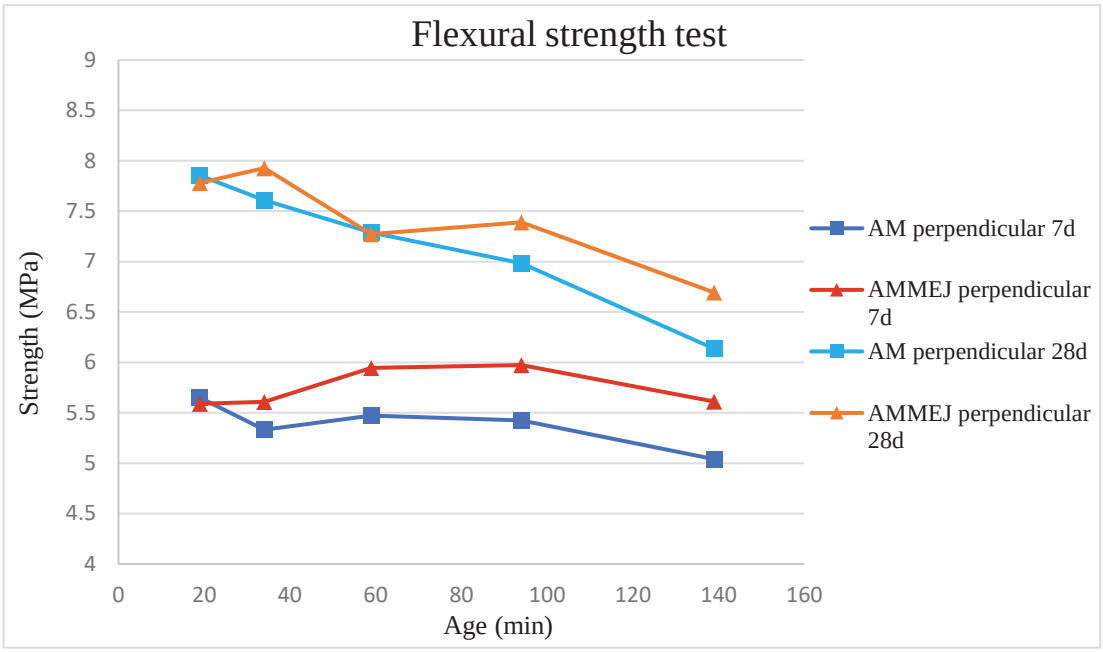

Figure 46. Experimental results for flexural strength test perpendicular to the casting direction.

By looking at the graph, it can be appreciated that, as expected, the mortar at age 28 days old presents higher strength than the mortar at age 7 days old. As the mortar's age increases, strength does it too.

Besides, unexpected, inside each range of age, the mortar using sand mussel shell has higher strength than conventional mortar. This is explained by the difference in shape between the conventional and mussel shell sand. The shape of conventional sand is crushed with all the dimensions similar while the shape of mussel shell sand is flaky type. This flaky shape may promote its orientation perpendicular to the applied load, acting as a reinforcement against tensile stresses generated in this kind of test.

Regarding the influence of the interlayer time, at age 7 days old the strength does not vary meanwhile at 28 days old, a decrease in the strength with time can be appreciated in both conventional and mussel mortar. At 7 days old the strength of the paste is low; therefore, the influence of the interlayer bond strength is not significant. At 28 days old, after a significant strength gain, this interlayer bond strength became important and therefore, as the time between casting layer increases, the bond strength decreases leading to decrease the mortar flexural strength. The influence is similar in both conventional and mussel mortar.

5.8.2 Compressive strength tests.

The means for compressive strength were calculated with the experimental data the same way as for flexural strength but in this case, there were 4 values for each point of the plot.

In *Figure 47*, it is shown the results for the conventional sand's mortar "AM" parallel and perpendicular to the casting direction at age 7 and 28 days old. In the same regard, the compressive strength test results for mortar using mussel shell sand "AMMEJ" perpendicular and parallel to the casting direction at ages 7 and 28 days old is shown in *Figure 48*.

These graphs show, as in flexural strength, that the compressive strength is higher at 28 days than at 7 days and that interlayer time is influencing the mortar strength more at 28 days than at 7 days. At 28 days it can be seen that as the interlayer time increases (interlayer bond strength decreases) the compressive strength decreases. Again, as in the flexural strength, the impact the interlayer bond strength is affecting conventional and mussel mortars in a similar way.

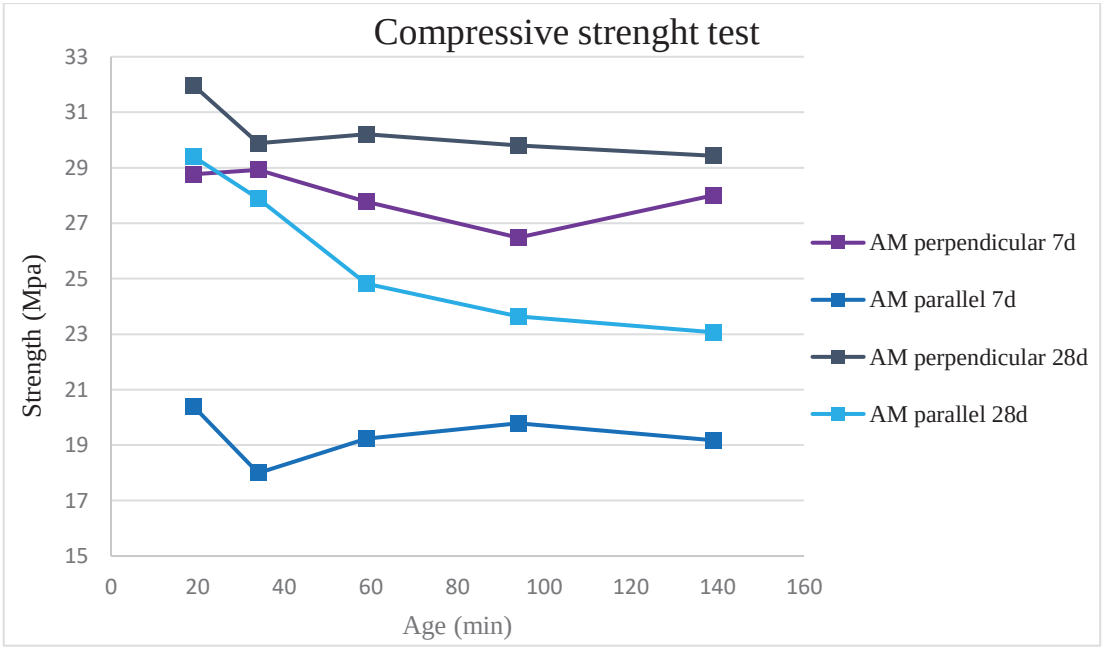

Figure 47. Experimental results for AM's compressive strength test.

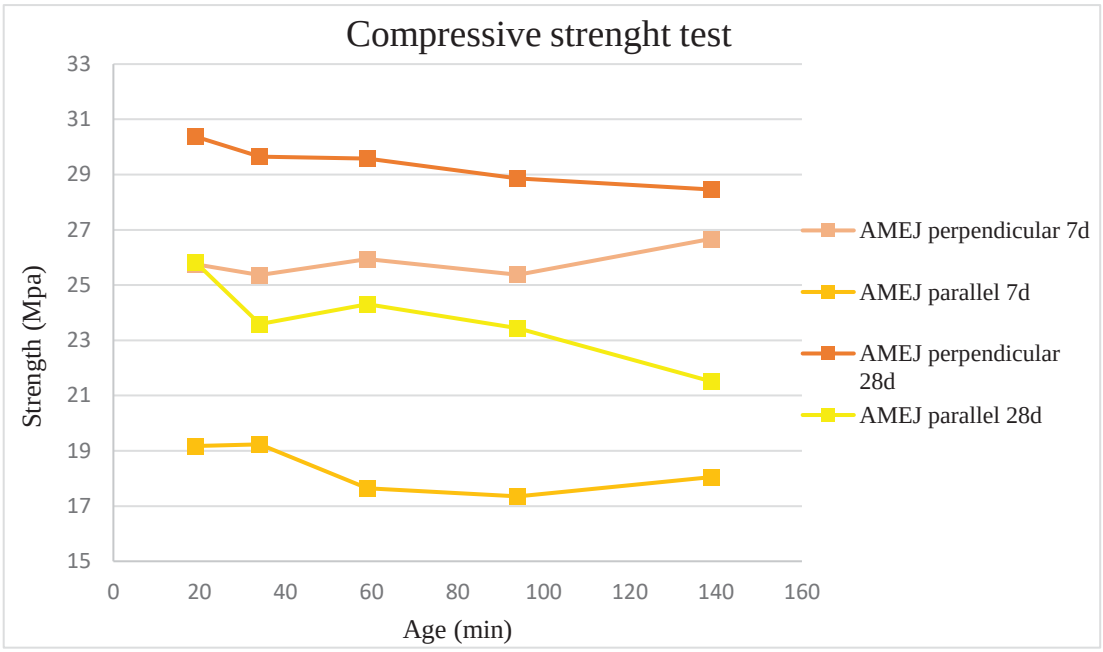

Figure 48. Experimental results for AMMEJ's compressive strength test.

The first layer was always filled up at age 19 min old meanwhile the second layer was filled at the stablished age (19, 34, 59, 94 and 139 min). As the period of time between filling up the first and second layer increased, more time had the first layer to set before adding the second one and therefore, the join between layers weakened. For that reason, as the difference in time in layer's filling increases, the strength upon breaking decreases. When mortar's age is 28 days old, the mortar layers reach a high strength, but the join between them is as weak as the beginning of the filling process so it makes the mortar break easier. However, when mortar's age is 7 days old, mortar layers do not get that high strength and the weak join between them does not influence in a higher extend.

In addition, in these graphs it can be appreciated that mortars tested perpendicular to cast direction (according to the standard) present greater values in strength than when they are tested parallel to cast direction.

The difference in strength between the mortars in perpendicular and parallel is related with the surface where the load is applied. When the mortars are sited perpendicular, the load is applied homogenously over a flat surface. However, when the mortars are placed parallel, the load is applied on the levelled face, so the irregularities present on the surface introduce tensile stress and therefore, the maximum stress obtained in the test is reduced.

5.9 Density.

The density of the two types of mortar ("AM" and "AMMEJ") fabricated in the laboratory to perform the experiments was calculated at their fresh state and at ages 1, 7 and 28 days old. The mass was obtained by weighting the test specimens, which dimensions were 4x4x16 cm (quadrangular prisms), used for the compressive strength tests.

Mortar's density depends on the density of the components used to fabricate it as well as its granulometry. Moreover, it is important the relation water/cement because as this relation increases, more porous will become the mortar. The theoretical density for settle mortar was calculated by knowing the mass and volume of each component of the mortar and the results were 1.954 g/cm^3 for conventional mortar and 1.960 g/cm^3 for mussel's mortar. Both densities are quite similar because the unique partial change in their composition is the type of sand and the difference in its density is insignificant: 2,670 g/cm^3 for conventional sand and 2.672 g/cm^3 for mussel shell sand. The graph below *(Figure 49)* shows the experimental densities obtained:

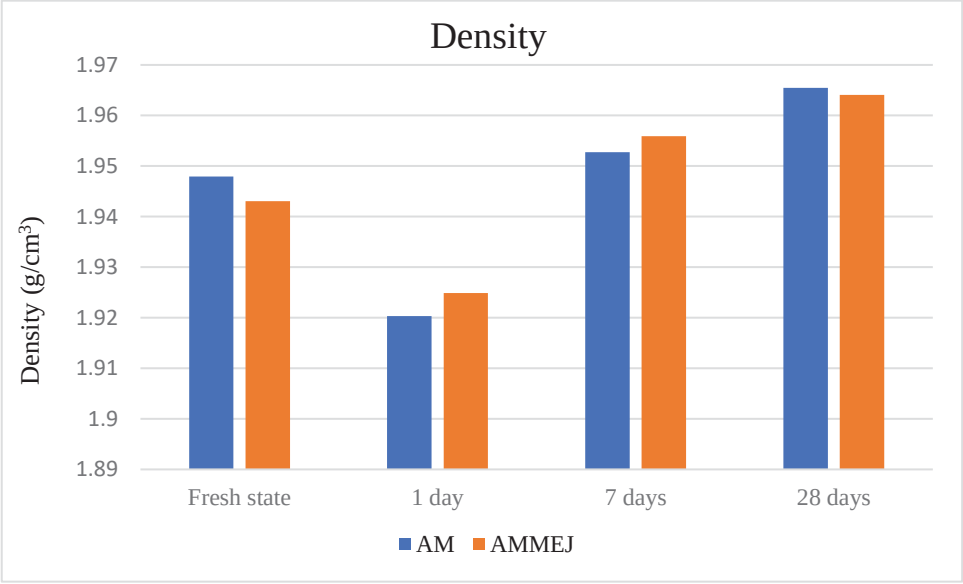

Figure 49. Mortars' densities at different ages.

Density in fresh state is first calculated, then the moulds were introduced in the climatic chamber that is a 50% humidity and although they were covered, it is clear that they lose water. That is why the density of the mortar at age 1 day old is the lowest one. Then, at 1 day old, the specimens were demoulded and introduced in water, which means 100% humidity. Therefore, the holes in their structure were occupied by water molecules, so at

age 7 and 28 days old, they presented higher density than the mortar at 1 day old. In addition, at these ages, both conventional and mussel mortars presented a density value similar to the theoretical one.

6. Conclusions/Conclusiones/Conclusións.

6.1 Conclusions.

According to the results obtained, the following conclusions can be drawn:

It is possible to fabricate a mussel mortar with the mussel sand obtained in the cannery industry. The mixing procedures can be similar to the ones developed with the conventional mortars and there won't be necessary to adapt the mortar plants if this by-product is being used.

The particle shape of the mussel sand is increasing the dynamic yield stress of the mussel mortars at early ages, therefore, its flowability and extrudability is going to be more difficult than in the conventional mortars. At long ages, the particle shape joint to the slow hydration rate of the mussel mortars, leads them to present similar dynamic yield stress which implies that they will present similar buildability.

Regarding viscosity, mussel sand incorporates always a low amount of fine particles (those under 63 microns) which means that, in general, mussel mortars are going to present lower viscosity values than conventional ones.

The results of the static yield stress are analogous in mussel mortars and conventional mortars and its evolution with time is also very similar. This means that both mortars present similar thixotropic behaviour.

According to the penetration test both conventional and mussel mortar evolve with time in a similar way. This means, again, that they both are going to present similar behaviour regarding buildability. However, in this case, it seems that the consistency (inverse of flowability) of mussel mortar is always higher (lower flowability) than the one of conventional mortar. However, according to the dynamic yield stress this is only true at early ages, where the differences in this penetration test are higher. At long ages the difference is only due to the particle shape. This test has to be used in combination with other when the aggregate shape is very flaky or angular (as it is in this case)

The results of the open time agree with the previous ones. Both conventional and mussel mortar evolve with time in a similar way and present similar strength values at any age

as this test is hardly sensitive to the particle shape. Again, it is recommended to use it in combination with others (especially with aggregates with flaky particles).

Shape retention results also agree with the previous ones. Similar results were found for "AM" and "AMMEJ" mortars, only differing at early ages where mussel shell mortars present higher values in SRF. Again, the presence of organic matter and especially the mussel shells shape justify these results.

The green strength results have shown considerable differences between mussel and conventional mortars. The retardation in the hydration process and the particle shape (that makes particles difficult to be surrounded or wrapped by the paste) decrease the green strength, specially at long ages, when this strength is going to be needed due to the successive layers.

The interlayer time (time between layer) is influencing the flexural strength of the mortars at long ages (at 28 days). At early ages (7 days), as the flexural strength of the mortar is low, the impact of this parameter is neglectful. The interlayer bond strength is affecting conventional and mussel mortars in a similar way (which again agree with the results of similar thixotropy). The same behaviour can be appreciated when compressive strength is analysed.

Regarding the influence of the load application in the test (perpendicular or parallel to the cast direction), it can be concluded that, when load is applied perpendicular (according to the standard) the compressive strength is always higher than when it is applied parallel (over the levelled face). The influence is similar in conventional and mussel mortars.

The density values of both conventional and mussel mortars were similar and, after soaking the specimens in water for curing, they presented similar values to the theoretical one (differences were only due to the difference in the density value of mussel sand when comparing it to the conventional sand).

As a final conclusion, both conventional and mussel mortar present a similar behaviour for 3D printing. The particle shape of the mussel shells and the presence of organic matter are the main factors that lead mussel mortars to present lower flowability at early ages and lower green strength at long ages. Due to this behaviour, the use of mussel shells will probably require the incorporation of more additives than the use of conventional sands.

6.2 Conclusiones.

De acuerdo con los resultados obtenidos, se pueden extraer las siguientes conclusiones:

Es posible fabricar un mortero de mejillón con la arena de mejillón obtenida en la industria conservera. Los métodos de mezcla pueden ser similares a los desarrollados con los morteros convencionales y no será necesario adaptar las plantas de mortero si se utiliza este subproducto.

La forma de las partículas de la arena de mejillón aumenta la tensión de flujo umbral dinámica de los morteros de mejillón a edades tempranas, por lo que su fluidez y capacidad de extrusión va a ser más difícil que en los morteros convencionales. A largas edades, la forma de la partícula unida a la lenta velocidad de hidratación de los morteros de mejillón, hace que presenten una tensión de flujo umbral dinámica similar, lo que implica que presentarán una constructibidad similar.

En cuanto a la viscosidad, la arena de mejillón incorpora siempre una baja cantidad de partículas finas (las inferiores a 63 micras) lo que significa que, en general, los morteros de mejillón van a presentar valores de viscosidad inferiores a los convencionales.

Los resultados de la tensión de flujo umbral estática son análogos en los morteros de mejillón y en los morteros convencionales y su evolución con el tiempo es también muy similar. Esto significa que ambos morteros presentan un comportamiento tixotrópico similar.

Según el ensayo de penetración, tanto el mortero convencional como el de mejillón evolucionan con el tiempo de forma similar. Esto significa, de nuevo, que ambos van a presentar un comportamiento similar en cuanto a la constructibidad. Sin embargo, en este caso, parece que la consistencia (inversa de la fluidez) del mortero de mejillón es siempre mayor (menor fluidez) que la del mortero convencional. Sin embargo, según la tensión de flujo umbral dinámica, esto sólo es cierto a edades tempranas, donde las diferencias en este ensayo de penetración son mayores. A edades largas, la diferencia se debe únicamente a la forma de las partículas. Este ensayo tiene que ser utilizado en combinación con otros cuando la forma del árido es muy plana o angular (como es en este caso).

Los resultados del tiempo abierto coinciden con los anteriores. Tanto el mortero convencional como el de mejillón evolucionan con el tiempo de forma similar y presentan valores de resistencia similares a cualquier edad ya que este ensayo es poco sensible a la forma de las partículas. De nuevo, se recomienda su uso en combinación con otros (especialmente con áridos con partículas planas y angulosas).

Los resultados de retención de forma también coinciden con los anteriores. Se encontraron resultados similares para los morteros "AM" y "AMMEJ", sólo difiriendo a edades tempranas donde los morteros de concha de mejillón presentan valores más altos en SRF. De nuevo, la presencia de materia orgánica y especialmente la forma de las conchas de mejillón justifica estos resultados.

Los resultados de resistencia en fresco han mostrado diferencias considerables entre los morteros de mejillón y los convencionales. El retardo en el proceso de hidratación y la forma de las partículas (que dificulta que sean rodeadas o envueltas por la pasta) disminuyen la resistencia en fresco, especialmente a largas edades, cuando ésta va a ser necesaria debido a las sucesivas capas.

El tiempo entre capas está influyendo en la resistencia a la flexión de los morteros a edades largas (a los 28 días). A edades tempranas (7 días), como la resistencia a la flexión del mortero es pequeña, el impacto de este parámetro es despreciable. La fuerza de unión entre capas afecta de forma similar a los morteros convencionales y a los de mejillón (lo que coincide de nuevo con los resultados de tixotropía similar). El mismo comportamiento se aprecia cuando se analiza la resistencia a la compresión.

En cuanto a la influencia de la aplicación de carga en el ensayo (perpendicular o paralela a la dirección hormigonado), se puede concluir que, cuando la carga se aplica perpendicularmente (según la norma) la resistencia a la compresión es siempre mayor que cuando se aplica paralelamente (sobre la cara enrasada). La influencia es similar en los morteros convencionales y de mejillón.

Los valores de densidad tanto de los morteros convencionales como de los de mejillón fueron similares y, tras la inmersión de las probetas en agua para su curado, presentaron valores similares al teórico (las diferencias se debieron únicamente a la diferencia en el valor de densidad de la arena de mejillón al compararla con la arena convencional).

Como conclusión final, tanto el mortero convencional como el de mejillón presentan un comportamiento que los hace adecuados para la impresión 3D. La forma de las partículas de las conchas de mejillón y la presencia de materia orgánica son los principales factores que introducen diferencias en su comportamiento. Estos parámetros hacen que los morteros de mejillón presenten una menor fluidez a edades tempranas y una menor resistencia en fresco a edades largas. Debido a ello, el uso de conchas de mejillón requerirá probablemente de la incorporación de más aditivos que en el caso de usar arenas convencionales.

6.3 Conclusións.

Segundo os resultados obtidos, pódense extraer as seguintes conclusións:

É posible facer un morteiro de mexillón con area de mexillón obtida na industria conserveira. Os métodos de mestura poden ser similares aos desenvoltos cos morteiros convencionais e non será necesario adaptar as plantas de morteiro se se utiliza este subproduto.

A forma das partículas de area de mexillón aumenta a tensión de fluxo limiar dinámico dos morteiros de mexillón a unha idade temperá, polo que a súa fluidez e capacidade de extrusión serán máis difíciles que nos morteiros convencionais. A longas idades, a forma da partícula, xunto coa lenta velocidade de hidratación dos morteiros de mexillón, fai que presenten unha tensión de fluxo limiar dinámica similar, o que implica que presentarán unha construtibidade similar.

En canto á viscosidade, a area do mexillón sempre incorpora unha cantidade baixa de partículas finas (menos de 63 micras), o que significa que, en xeral, os morteiros de mexillón presentarán valores de viscosidade inferiores aos convencionais.

Os resultados do tensión de fluxo limiar estático son similares en morteiros de mexillón e en morteiros convencionais e a súa evolución no tempo tamén é moi similar. Isto significa que ambos morteiros teñen un comportamento tixotrópico similar.

Segundo a proba de penetración, tanto o morteiro convencional como o mexillón evolucionan de xeito similar co paso do tempo. Isto significa, de novo, que ambos

presentarán un comportamento similar en termos de construtibidade. Non obstante, neste caso, parece que a consistencia (inversa da fluidez) do morteiro de mexillón é sempre maior (menos fluidez) que a do morteiro convencional. Non obstante, segundo a tensión de fluxo limiar dinámico, isto só é certo en idades temperás, onde as diferenzas nesta proba de penetración son maiores. A longas idades, a diferenza débese unicamente á forma das partículas. Esta proba ten que usarse en combinación con outras cando a forma do árido é moi plano ou angular (como é neste caso).

Os resultados do tempo aberto coinciden cos anteriores. Tanto o morteiro convencional coma o de mexillón evolucionan de xeito similar co paso do tempo e presentan valores de resistencia similares a calquera idade xa que esta proba non é moi sensible á forma das partículas. De novo recoméndase o seu uso en combinación con outros (especialmente con áridos con partículas planas e angulosas).

Os resultados de retención de formas tamén coinciden cos anteriores. Atopáronse resultados similares para os morteiros "AM" e "AMMEJ", só difiren en idades temperás onde os morteiros de cuncha de mexillón mostran valores SRF máis altos. De novo, a presenza de materia orgánica e especialmente a forma das cunchas de mexillón xustifica estes resultados.

Os resultados de resistencia en fresco mostraron diferenzas considerables entre os morteiros de mexillón e os morteiros convencionais. O atraso no proceso de hidratación e a forma das partículas (o que dificulta que sexa rodeadas ou envoltas pola pasta) diminúen a resistencia cando están frescas, especialmente a longas idades, cando será necesario debido ás sucesivas capas.

O tempo entre capas está a influír na resistencia á flexión dos morteiros en idades longas (aos 28 días). En idades temperás (7 días), como a resistencia á flexión do morteiro é pequena, o impacto deste parámetro é insignificante. A resistencia de unión entre capas afecta de xeito similar ao morteiro convencional e ao mexillón (que coincide de novo cos resultados dunha tixotropía similar). O mesmo comportamento pódese ver cando se analiza a resistencia á compresión.

En canto á influencia da aplicación de carga na proba (perpendicular ou paralela á dirección de hormigonado), pódese concluír que, cando a carga se aplica perpendicularmente (segundo o estándar), a resistencia á compresión é sempre maior que

cando se aplica en paralelo (na cara enrasada). A influencia é similar nos morteiros convencionais e de mexillóns.

Os valores de densidade tanto dos morteiros convencionais coma dos mexillóns foron similares e, despois de mergullar os exemplares en auga para curalos, presentaron valores similares ao teórico (as diferenzas só foron debidas á diferenza no valor de densidade da area de mexillón cando se compara coa area convencional).

Como conclusión final, o morteiro convencional e o mexillón mostran un comportamento que os fai axeitados para a impresión 3D. A forma das partículas da cuncha de mexillón e a presenza de materia orgánica son os principais factores que introducen diferenzas no seu comportamento. Estes parámetros fan que os morteiros de mexillón presenten unha menor fluidez a idades temperás e una menos resistencia en fresco a idades longas. Debido a isto, o uso de cunchas de mexillón probablemente requirirá a incorporación de máis aditivos que no caso de usar areas convencionais.

7. Future lines of investigation.

As it was mentioned before, possible further research could be about the incorporation of more additives, and the choose of those additives, in mussel shell sand mortar as well as the proper percentage of mussel shell sand (perhaps lower than the used in this work) in the mixtures, to obtain more flowability at early ages and higher green strength at long ages.

In addition, a suitable method to measure green strength would be interesting to accomplish in future works due to the lack of vertical displacement showed in the experimental procedure.

Finally, the performance of proper extrusion tests to evaluate the flowability and extrudability of mortar is recommended.

8. Timeframe.

MONTH	WORK
MARCH	Laboratory work
APRIL	Laboratory work
MAY	Laboratory work and TFG script
JUNE	Laboratory work and TFG script
JULY	TFG script
AUGUST	Last week of August: TFG script
SEPTEMBER	From day 1 to 10: Final modifications of the TFG.

9. Bibliography.

1. Callister, W. D. Materials science and engineering: an introduction. John Wiley & Sons, 2007.

2. Norma Española. UNE-EN 197-1. Cemento. Parte 1: Composición, especificaciones y criterios de conformidad de los cementos comunes. 2011.

3. Universidad de A Coruña. E.T.S.I Caminos Canales y Puertos. Slides: "Ligantes: Cementos".https://www.docsity.com/es/ligantes-cementos-materiales-de-construccion-apuntes/156708/ (Date of access: 20/6/21)

4. Khatib, J. M., Baalbaki, O. & ElKordi, A. Metakaolin. Waste and Supplementary Cementitious Materials in Concrete: Characterisation, Properties and Applications 493–511 (Elsevier, 2018).

5. Martínez-García, C.; González-Fonteboa, B.; Carro-López, D.; Martínez-Abella, F. Impact of mussel shell aggregates on air lime mortars. Pore structure and carbonation. Journal of cleaner production 2019, 215, 650-668.

6. Martínez García, C. Estudio del comportamiento de la concha de mejillón como árido para la fabricación de hormigones en masa: aplicación en la cimentación de un módulo experimental (Módulo Biovalvo), (Traballo de Fin de Grado) Universidad de A Coruña.2016.

7. Rodríguez Álvaro Roberto. Morteros para revestimiento con árido procedente de concha de mejillón, (Trabajo de Fin de Grado) Universidad de A Coruña. 2014.

8. Génio L., Cunha MR., Grahame J. Shell microstructures of mussels (Bivalvia Mytilidae Bathymodiolinae) from deep-sea chemosynthetic sites: Do they have a phylogenetic significance? Little CTS. 2014, Deep Sea Res Part I Oceanogr Res, págs. 86-103.

9. Hahn, S. Exploring aberrant bivalve shell ultrastructure and geochemistry as proxies for past sea water acidification. Sedimentology, 2014, 61,1625-1658.

10. Hahn, S. Marine bivalve shell geochemistry and ultrastructure from modern low pH environments: environmental effect versus experimental bias. 2011, p. 1897-1914.

11. Xunta de Galicia. Consellería do mar. https://mar.xunta.gal/gl/o-mar/o-sector/acuicultura. (Date of access:10/6/21).

12. Ministerio de Agricultura Pesca y Alimentación. Gobierno de España. Acuivisor. https://servicio.pesca.mapama.es/acuivisor/. (Date of access: 10/6/21).

13. Marin, F; L. G. Molluscan shell proteins. Camptes Rendus Paleovol. 2004, p. 469–492.

14. Salgado Beceiro, J. Deseño e estudo reolóxico de materiais cerámicos para impresión 3D. (Trabajo de Fin de Máster) Universidad de A Coruña.2018.

15. Bentz, D. P., Jones, S. Z., Bentz, I. R. & Peltz, M. A. Towards the formulation of robust and sustainable cementitious binders for 3-D additive construction by extrusion. Construction and Building Materials, 2018, 175, 215–224.

16. Universidade da Coruña. E.T.S.I de Caminos, Canales y Puertos. Slides: "Reología de materiales base cemento". Authors: Fernando Martínez Abella, Belén González Fonteboa and Gemma Rojo López. (Internal document).

17. González-Taboada, I., González-Fonteboa, B., Martínez-Abella, F. & Seara-Paz, S. Thixotropy and interlayer bond strength of self-compacting recycled concrete. Construction and Building Materials 2018 161, 479-488.

18. Soltan, D. G.; Li, V. C. A self-reinforced cementitious composite for building-scale 3D printing. Cement & concrete composites 2018, 90, 1-13.

19. Marchon, D.; Kawashima, S.; Bessaies-Bey, H.; Mantellato, S.; Ng, S. Hydration and rheology control of concrete for digital fabrication: Potential admixtures and cement chemistry. Cement and Concrete Research 2018, 112, 96-110.

20. Norma Española. UNE-EN 413-2. Cementos de albañilería. Parte 2: Métodos de ensayo. 2017.

21. Norma Española. UNE-EN 1015-9. Métodos de ensayo de los morteros para albañilería. Parte 9: Determinación del periodo de trabajabilidad y del tiempo abierto del mortero fresco. 2000.

22. Sánchez, J. A., Químicas, O., Barrios, J. & Arquitectura, C. E. T. S. La retracción en los morteros de cal. Materiales de construcción, 1997, 47 (245), 17-28.

23. Norma Española. UNE-EN 169-1. Métodos de ensayo de cementos. Parte 1: Determinación de resistencias. 2018.

24. Ding, T., Xiao, J., Qin, F. & Duan, Z. Mechanical behavior of 3D printed mortar with recycled sand at early ages. Construction and Building Materials, 2020, 248, 1-11.